NOVA SCHOOL OF SCIENCE & TECHNOLOGY

DEPARTMENT OF LIFE SCIENCES

BRENDA GABRIELLA FRANÇA

BSc in BIOLOGICAL SCIENCES

THE ROLE OF POST-TRANSLATIONAL MODIFICATIONS ON NKX6-2 BEHAVIOR AND FUNCTION

MASTER IN MOLECULAR GENETICS AND BIOMEDICINE

NOVA University Lisbon

September, 2023

NOVA SCHOOL OF SCIENCE & TECHNOLOGY

DEPARTMENT OF LIFE SCIENCES

THE ROLE OF POST-TRANSLATIONAL MODIFICATIONS ON NKX6-2 BEHAVIOR AND FUNCTION

BRENDA GABRIELLA FRANÇA

BSc in BIOLOGICAL SCIENCES

Adviser: Federico Herrera

Assistant Professor, Faculdade de Ciências, Lisbon University

Co-advisers: Margarida Castro Caldas

Assistant Professor, NOVA School of Science and Technology, NOVA University Lisbon

Examination Committee:

Chair: **Maria Alexandra Núncio de Carvalho Ramos Fernandes,**

Associate Professor, NOVA School of Science and Technology, NOVA University Lisbon

Rapporteurs: **Sandra Cristina Henriques Vaz,**

Assistant Professor, Faculdade de Medicina, Lisbon University

Adviser: **Federico Herrera,**

Assistant Professor, Faculdade de Ciências, Lisbon University

MASTER IN MOLECULAR GENETICS AND BIOMEDICINE

NOVA University Lisbon

September, 2023

The role of post-translational modifications on NKX6-2 behavior and function

I dedicate this thesis to my dear siblings, Bruno and Bianca.

ACKNOWLEDGEMENTS

Upon completing this thesis, I would like to express my gratitude to the individuals and institutions involved who made this work possible.

I would like to thank my advisor, Dr. Federico Herrera, for the opportunity to work in his laboratory, for his patience, and for all the support provided.

I extend my appreciation to my co-advisor, Dr.ª Margarida Castro Caldas, for the support and attention provided during classes and the development of the thesis. I also wish to express my gratitude to all the professors of the Department of Life Sciences at the NOVA School of Science and Technology, who collectively contributed to my growth as a scientist.

To my colleagues at the Cell Structure and Dynamics Laboratory, especially André Costa, Pedro Peralta, Fernanda Murtinheira, Carina Coelho, Ana Sofia and Constança Pimenta, my heartfelt thanks for all the care, patience, assistance, companionship, and support during the period we worked together. Thank you for making this period of intense pressure lighter and happier.

I would like to thank my closest friends, especially Yasmim, Guilherme, Aline and Reyner, for always listening to me and assisting in your own ways.

Lastly, I want to express my gratitude to my family who lives with me and supported me from the first moment, but especially my parents and siblings, whom I left in Brazil and went in search of further learning in another country, to live and complete this important stage of my life and career. Thank you for all the support and understanding throughout my life.

"No great discovery was ever made without a bold guess." (Isaac Newton).

ABSTRACT

NK6 Homeobox 2 (NKX6-2) is a member of the NKX family of transcriptional regulators, responsible for governing oligodendrocyte maturation and the fate of motor neurons and pancreatic cells. Loss-of-function mutations in the NKX6-2 gene result in a rare autosomal recessive genetic disorder known as Spastic Ataxia (SPAX8) with hypomyelinating leukodystrophy. This disease is characterized by cerebellar dysfunction, loss of white matter and, in some cases, atrophy of the vermis and cerebellar hemispheres. Some of the mutations on NKX6-2 affect a putative transactivation domain (TAD), located at the C-terminus of the protein and which function is unclear. Consultation of public databases indicate that TAD contains three residues that have been found phosphorylated in high-throughput mass spectrometry analyses: S246, T252 and Y238. However, the function of these phosphorylation events remains completely unknown. This study attempted to address a fundamental question related to the role of post-translational modifications on the intracellular location of NKX6-2. We have developed mammalian expression constructs encoding NKX6-2 fused to the Venus fluorescent reporter, where the transcription factor carries point mutations that inhibit and mimic phosphorylation at S246, T252, and Y238. Specifically, mutating S246 and T252 to alanine, and Y238 to phenylalanine, would prevent their phosphorylation while keeping similar structure. On the other hand, mutating S246 and T252 to aspartic acid added an extra negative charge at these sites, partially mimicking phosphorylation. The tyrosine residue was not mutated to mimic phosphorylation, because there are no natural amino acids with an extra negative charge that share the phenolic ring of tyrosine. No mutation produced alterations in the nuclear localization of NKX6-2 in living cells. However, mutations in this protein were associated with nuclear morphology abnormalities, as well as increased protein stability. Additionally, we identified endogenous expression of NKX6-2 in human cancer cell lines where we could study NKX6-2 in normal and pathological, SPAX8-related conditions. These results offer crucial insights into molecular and cellular aspects of NKX6-2 biology, with potential implications for SPAX8.

Keywords: NKX6-2; Transcription factor; Spastic ataxia 8; Phosphorylation; Transactivation domain.

RESUMO

NK6 Homeobox 2 (NKX6-2) é um membro da família NKX de reguladores transcricionais, responsável por controlar a maturação de oligodendrócitos e o destino de neurónios motores e células pancreáticas. Mutações de perda de função no gene NKX6-2 resultam numa rara doença genética autossómica recessiva conhecida como Ataxia Espástica 8, em inglês: Spastic Ataxia 8 (SPAX8) com leucodistrofia hipomielinizante. Esta doença é caracterizada por disfunção cerebelar, perda de substância branca e, em alguns casos, atrofia do vermis e dos hemisférios cerebelares. Algumas das mutações em NKX6-2 afetam um domínio de transativação putativo (TAD), localizado no C-terminus da proteína, cuja função é incerta. Consultas em bases de dados públicas indicam que o TAD contém três resíduos que foram encontrados fosforilados em análises de espectrometria de massa de alta resolução: S246, T252 e Y238. No entanto, a função desses eventos de fosforilação permanece completamente desconhecida. Este estudo procurou abordar uma questão fundamental relacionada com o papel das modificações pós-traducionais na localização intracelular do NKX6-2. Desenvolvemos construções de expressão em mamíferos codificando o NKX6-2 fundido com o marcador fluorescente Venus, em que o fator de transcrição transporta mutações pontuais que inibem e imitam a fosforilação em S246, T252 e Y238. Especificamente, a mutação de S246 e T252 para alanina e Y238 para fenilalanina impediria a sua fosforilação, mantendo uma estrutura semelhante. Por outro lado, a mutação de S246 e T252 para ácido aspártico adicionou uma carga negativa extra nesses locais, imitando parcialmente a fosforilação. O resíduo de tirosina não foi mutado para imitar a fosforilação, porque não existem aminoácidos naturais com uma carga negativa extra que partilhem o anel fenólico da tirosina. Nenhuma mutação produziu alterações na localização nuclear do NKX6-2 em células vivas. No entanto, mutações nesta proteína foram associadas a anomalias na morfologia nuclear, bem como a um aumento na estabilidade da proteína. Além disso,identificámos a expressão endógena do NKX6-2 em linhas celulares de cancro humano, onde pudemos estudar o NKX6-2 em condições normais e patológicas relacionadas com o SPAX8.
Estes resultados oferecem informações cruciais sobre aspetos moleculares e celulares da biologia do NKX6-2, com possíveis implicações para o SPAX8.

Palavras-chave: NKX6-2; Fator de transcrição; Ataxia Espástica 8; Fosforilação; Domínio de Transativação.

CONTENTS

LIST OF FIGURES

LIST OF TABLES

ACRONYMS

A	Alanine
ARSACS	Autosomal Recessive Spastic of Charveloix-Saguenay
BSA	Bovine Serum Albumin
CNS	Central Nervous System
D	Aspartic Acid
DMEM	Dulbecco Modified Eagle Medium
DNA	Deoxyribonucleic Acid
dNTP	Deoxynucleotide Triphosphates
DTT	Dithiothreitol
ECL	Enhanced Chemiluminescence
EDTA	Ethylenediaminetetra-acetic Acid
F	Phenylalanine
G	Glycine
GAPDH	Glyceraldehyde-3-phosphate Dehydrogenase
Gtx	Glia- and -testis-specific homeobox gene
HEPES	4-(2-hydroxyethyl)-1-piperazineethanesulfonic Acid
IN	Interneurons
K	Lysine
kDa	Kilodalton
LB	Luria Broth
LIMK2	LIM Domain Kinase 2
MAPK	Mitogen-activated Protein Kinase

MBP	Myelin Basic Protein
MN	Motor Neurons
NaCl	Sodium Chloride
NGS	Next-Generation Sequencing
NKX	NK Homeobox
PBS	Phosphate-Buffered Saline
PCNA	Proliferating Cell Nuclear Antigen
PCR	Polymerase Chain Reaction
PDEF	Prostate-derived Ets Factor
PLP1	Proteolipid Protein 1
PP	Phosphatase
PTMs	Post-translational modifications
RNA	Ribonucleic Acid
rpm	Revolutions per Minute
S	Serine
SCA	Spinocerebellar ataxias
SDS	Sodium Dodecyl Sulfate
Shh	Sonic Hedgehog Signaling
SPAX8	Spastic Ataxia 8
T	Threonine
TAD	Transactivation Domain
TBS	Tris-Buffered Saline
TBS-T	Tris-Buffered Saline with Tween 20
TTF-1	Thyroid Transcription Factor-1
Wnt	Wingless-related Integration Site
WT	Wild Type
Y	Tyrosine

SYMBOLS

-	When associated with graphs, it represents the absence of the protein.
*	When associated with amino acids it represents a STOP codon.
*	When associated with graphics it represents a P-value of a comparison between data (* <0,05; **<0,01; *** <0,001; **** <0,0001).

Part of the results of this thesis have been published in Ferreira-Peralta, P., França, B., Murtinheira, F., Rodrigues, M. S. & Herrera, F. (2023). Is spastic ataxia 8 a protein misfolding disorder? *Biochimica et Biophysica Acta (BBA) - Molecular Basis of Disease.* https://doi.org/10.1016/j.bbadis.2023.166882.

1

INTRODUCTION

1.1 The cerebellum

The cerebellum is a key structure in the central nervous system (CNS), derived from the rhombencephalon, located posterior to the IV cerebral ventricle, in the posterior fossa of the skull [1, 2]. It plays an important role in the coordination and balance of motor activity, as well as in cognition and processing sensory information from movement [3, 4, 5], among other CNS functions. Anatomically, the cerebellum is divided into two hemispheres connected by a structure called vermis and separated into three lobes by three main fissures. The primary or anterior fissure divides the anterior and posterior lobes; the posterolateral fissure divides the flocculonodular lobe from the posterior lobe; and the horizontal fissure borders the superior and inferior surfaces of the cerebellum itself [1] (**Figure 1.1**). The lobes can be divided into the spino-cerebellum, ponto-cerebellum and vestibulo-cerebellum [6].

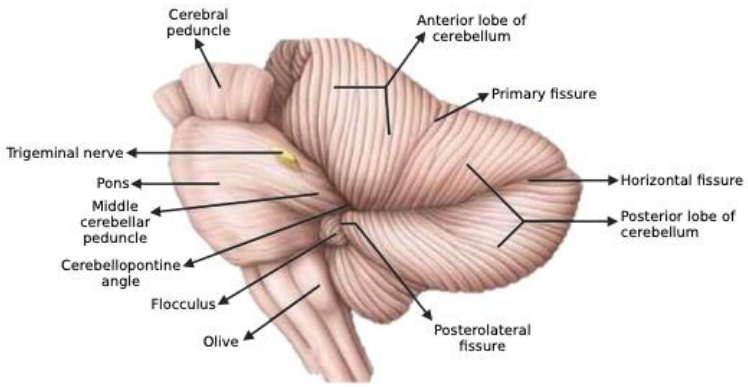

Figure 1.1 — Representative image of cerebellar divisions. Adapted from Schuenke, M., *et al.* [6], created with *BioRender.com*.

The cerebellum has a medullary body with an abundance of gray matter and a cortex that surrounds a white matter center, similar to the brain [7]. The white matter contains 4 pairs of deep cerebellar nuclei surrounded by the cerebellar cortex [8]. The medial nucleus is called the fastigial nucleus, the dentate nucleus corresponds to the lateral nucleus, and the globose and emboliform nuclei, which correspond to the anterior and posterior interbody, respectively, are called interposed nuclei [8] (**Figure 1.2**). These nuclei project efferent fibers to the brainstem nuclei [9].

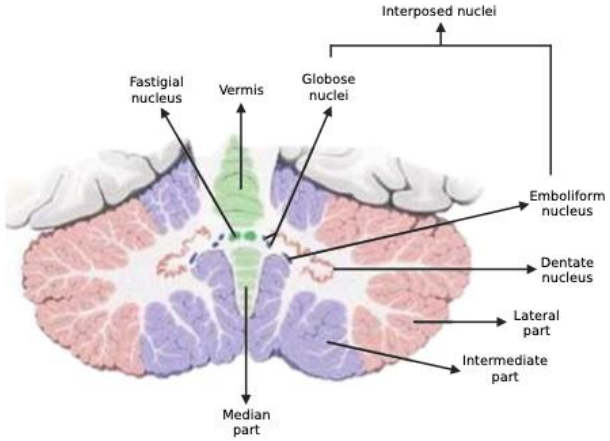

Figure 1.2 — Representation of the deep cerebellar nuclei. Adapted from Schuenke, M., *et al.* [6], created with *BioRender.com.*

Three pairs of cerebellar peduncles allow fibers to enter and exit the cerebellum: the inferior cerebellar peduncle connects the cerebellum to the spinal cord; the middle cerebellar peduncle transmits information about voluntary motor activities and connect it to the pons and the midbrain, with the aid of the superior cerebellar peduncle, which extends to outside the cerebellum at the exit of the trochlear nerve [10] (**Figure 1.3**).

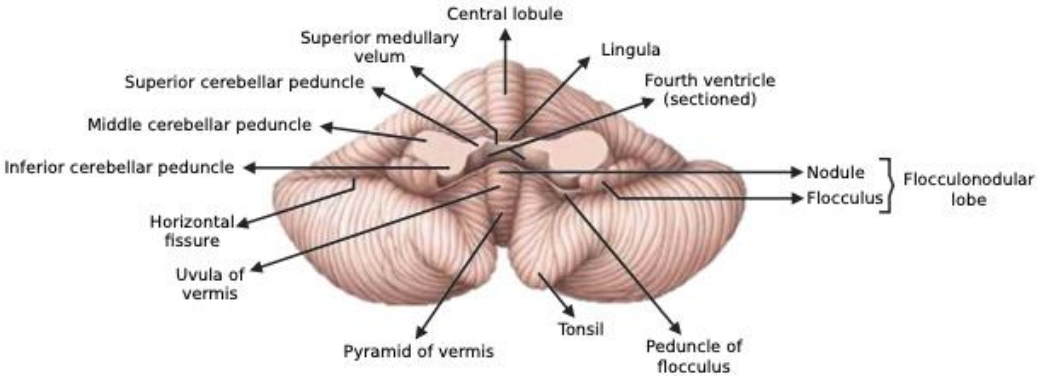

Figure 1.3 — Representation of the cerebellar peduncles. Adapted from Schuenke, M., *et al.* (2020) [6], created with *BioRender.com*.

Despite occupying only 10% of the brain volume, approximately 60% of all brain neurons are contained in the cerebellum, organized into six main neuronal populations: Purkinje, Lugaro, stellate cells, Golgi, basket and granule cells [2]. Most of the major neuronal cells mentioned are GABAergic, i.e. inhibitory, except for the granular cells which are glutamatergic, i.e. excitatory [11, 12]. The cerebellum receives sensory information from the afferent fibers and the principal afferent pathways are the climbing and mossy fibers, which are excitatory and interconnect different regions [13]. These fibers form complex connections with the Purkinje cells and granular cells that exert an excitatory effect before penetrating the white matter. The climbing fibers move independently during development through the layers of cortex and wrap around the dendrites of Purkinje cells while the mossy fibers are highly branched and stimulate inhibitory interneurons, granular cells, cerebellar nuclei and Purkinje cells [13, 14]. Basket, stellate, and Golgi cells can limit the excited area and control the amount of excitation brought to the Purkinje cells by the climbing and mossy cells because they are inhibitory neurons [15]. The fastigial, dentate and interposed nuclei all project efferent fibers that have an impact on both motor and non-motor activities, such as the processing of emotions and thoughts [11, 13]. The cerebellar cortex is formed by the inner, middle and outer layers. The inner layer is composed of granular cells and Golgi cells. The middle layer is mainly composed of Purkinje cells, which are the only efferent neurons of the cerebellar cortex, responsible for inhibiting neurons in the deep cerebellar nuclei. Bergmann's glia is also found in this layer, these specialized astrocytes being closely linked to the Purkinje cells. Finally, the outer molecular layer is mainly composed of stellate and basket cells [14] (**Figure 1.4**).

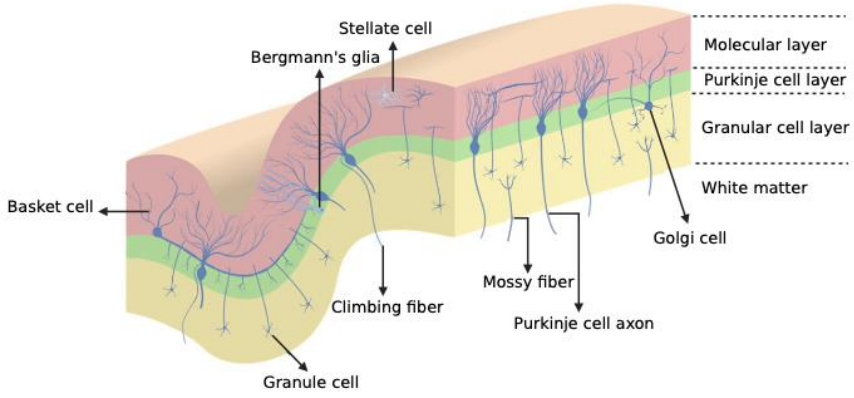

Figure 1.4 — Layers of the cerebellar cortex. Image adapted from *https://www.lecturio.com/pt/concepts/cerebelo-anatomia/* (2020) and created with *BioRender.com*.

There are three arteries responsible for the irrigation of the cerebellum, namely: the superior cerebellar artery, the anterior inferior cerebellar artery and the posterior inferior cerebellar artery. The superior cerebellar artery irrigates the trigeminal nerve, dentate nucleus, superior vermis, part of the midbrain and cerebellar white matter [15]. It can be associated with the development of aneurysms, ischemic syndromes and neurovascular compressions, such as oculomotor nerve palsy, hemifacial spasm and ocular neuromyotonia [15]. The anterior inferior cerebellar artery has a variable course, and may anastomose with other arteries, in addition to giving rise to the labyrinthine artery, which irrigates the inner ear [16]. In this artery, aneurysms are very rare and represent less than 1% of all existing intracranial aneurysms [16]. Finally, the posterior inferior cerebellar artery, which is the largest branch of the vertebral artery, and irrigates the cerebellar tonsils, the gracilis nucleus of the medulla and the caudal medulla, among others [17]. The occlusion of this artery can cause serious sequelae, ranging from silent ischemic injury, edema, hemorrhage, brainstem infarction and death [17].

The cerebellum uses a mechanism for movement control, divided between movement planning and movement correction in execution. Movement initiation is controlled by the spinocerebellum, which compares the characteristics of the movement in execution with the motor plan, formulates the corrections and adjusts whatever is necessary to carry out the movement [18]. The dentate nucleus is activated before the onset of movement and the interpositus nucleus after the movement begins, as it is involved in movement correction [13]. Just as the cerebellum regulates strength, precision of movement, muscle tone, balance, speed and rhythm, it is also able to control consistency, some types of non-motor cognition and the speed of cognitive processes, such as memory, language, visuoconstructive skills, attention and locomotor learning [19]. Cerebellar dysfunction can happen at any stage of life and normally cause alterations in body and eye movements and balance, usually resulting in a characteristic type of uncoordinated movement known as ataxia [20]. Symptoms of cerebellar damage are varied and can include posture and gait disturbances, behavioral abnormalities of higher functions, loss of balance, irregular steps, speech changes and tremors.

1.1.1 Ataxias

Ataxias are a group of neurodegenerative diseases characterized by irregular movements, lack of motor coordination, hypotonia, asynergy, excessive tremor, gait abnormality, dysarthria, and impaired balance [21]. Hereditary ataxias are genetic and passed down

through families. Some ataxias begin during childhood or adolescence, such as Spastic Ataxia 8 (SPAX8) and Autosomal Recessive Spastic Ataxia of Charveloix-Saguenay (ARSACS), leading to progressive symptoms over time, while others begin in adulthood, such as spinocerebellar ataxias or Machado-Joseph disease [22]. These ataxias can have mitochondrial inheritance, linked to X and autosomal recessive or dominant. Since initial diagnosis is sometimes difficult due to similarities between the symptoms of the different ataxias [22], genetic testing often needs to consider family history and age [22]. In contrast to the dominantly inherited spinocerebellar ataxias, or SCAs, recessive ataxias do not have a common abbreviation for classification. The term autosomal recessive spinocerebellar ataxia (SCAR) was assigned based on the discovery of the locus and has been used to designate new recessive ataxias, but this nomenclature does not include the most frequent or previously described ataxias. The term spastic ataxia (SPAX) has also been used to describe ataxias with significant spasticity, regardless of inheritance pattern [23]. Acquired ataxias, on the other hand, are caused by non-genetic factors such as traumatic injuries, stroke, tumors, infections or toxins affecting the brain or cerebellum [24]. In older individuals with no family history for a particular ataxia, sporadic etiology becomes more likely. However, a negative family history or advanced age does not completely rule out hereditary ataxia, as they can also be caused by de novo mutations [21].

In the last decade, there has been great progress in the diagnosis of hereditary ataxias, due to application of next-generation sequencing (NGS) in clinical practice. This technique is based on the binding of single-stranded genetic material to a solid surface coated with adapter oligonucleotides, it is more sensitive and capable of reading many genes at the same time. However, it has high error rates when sequencing large amounts of genome and can identify new variants or other health conditions that the patient has and that are not related to the disease under study. There is still no consensus on the best approach for diagnosing ataxia: despite the usefulness of bioinformatic tools, they are still not able to provide a de-finitive answer without other functional studies, and the protocol is variable [25, 26].

Beyond genetic testing, some formal instruments are used to quantify motor deficit and disease progression in ataxias. Among the most widely used are the International Cooperative Ataxia Rating Scale [27], the Scale for the Assessment and Rating of Ataxia [28] and the Brief Ataxia Rating Scale [29]. The International Cooperative Ataxia Rating Scale was

developed to evaluate cerebellar ataxias and is the most used scale in pediatric studies due to its sensitivity from mild to severe cases, but it consists of 19 items and a 100-point scale, limiting its use because it is time-consuming. The Scale for the Assessment and Rating of Ataxia scale contains 8 items and 40 points, presents similar problems to the previous one, which makes it unfeasible in wider clinical practices due to the time spent using it [21]. Finally, the more recent scale created is the Brief Ataxia Rating Scale and is a briefer version of the International Cooperative Ataxia Rating Scale, reliable and easy to apply, having only a 30-point scale.

Ataxias can have different particularities depending on the location of the lesion. For example, midline lesions of the cerebellar vermis or flocculonodular lobes cause truncal ataxia, abnormal eye movements, nausea, vomiting, and vertigo, while lateral lesions typically result in appendicular or limb ataxia. Ataxia can also result from infarcts in the lateral medulla or pons because these structures are directly connected to the cerebellar peduncles [30]. It can also be a symptom of hereditary polyneuropathies, mitochondrial diseases, hereditary spastic paraplegias, and neurodevelopmental disorders, such as neuronal ceroid lipofuscinoses, Jourbert syndrome and recessive Behr's syndrome [31]. The phenotype of ataxias varies drastically across patients from different families as well as within the same family with the same mutated gene, depending upon the type of mutation, age of onset, location in the gene, the presence of modifying genes, and environmental exposures [23]. Recessive ataxias have more complex phenotypes than dominant ataxias, including pyramidal and extrapyramidal involvement, neurophaty, hypogonadism, cognitive involvement, seizures, retinopathy and many others [23].

Ataxias are rare disorders, but autosomal recessive ataxias are slightly more common (3.3/100,000 people) than autosomal dominant ataxias (2.7/100,000 people) [32]. Friedreich's ataxia and ataxia-telangiectasia are the most common autosomal recessive ataxias, while Machado-Joseph disease and spinocerebellar ataxia type 2 are the most common autosomal dominant ataxias [32]. Spain and France have the largest prevalence of autosomal recessive ataxias, while Portugal, Japan, and Norway have the highest prevalence of autosomal dominant ataxias [32]. In Portugal, the most prevalent autosomal ataxias are Machado-Joseph disease and dentatorubro-palidoluysian atrophy; and the most prevalent autosomal recessive ataxias are ataxia with oculomotor apraxia and Friedreich’s ataxia [33]. Machado-Joseph disease typically manifests after the age of 40, when the patient begins to show slow and progressive cerebellar ataxia associated with neuropathy and possible movement disorders [34]. The dentatorubro-palidoluysian atrophy has a wide range of onset ages with

younger patients having progressive myoclonic epilepsy associated with ataxia and older patients having chorea associated with ataxia [35]. Ataxia with oculomotor apraxia presents slowly progressive cerebellar ataxia in childhood, peripheral neuropathy, and oculomotor apraxia over the years [36]. Friedreich's ataxia begins between 10 and 16 years of age, and shows non-neurological symptoms, sensory ataxia, and neuropathy [37].

While the most frequent ataxias, being rare, have attracted much attention and funding support in the last decades, there are still many rarer ataxias that need further characterization at cellular and molecular levels. In this project, the ataxia addressed is called Spastic Ataxia 8 (SPAX8) [38].

1.1.2 SPAX8

Spastic ataxia 8 is a rare autosomal recessive neurodegenerative disorder characterized by loss of motor function in the first year of life and caused by loss-of-function mutations in the NK6 Homeobox 2 gene (NKX6-2) [39, 40]. The prognosis of patients can be classified into two types based on the age of onset. The severe type begins in the neonatal period and progresses rapidly, manifesting as nystagmus, severe spastic tetraplegia with joint contractures and scoliosis, hearing impairment, visual impairment, and death in early childhood [38]. On the other hand, the milder type is characterized by normal acquisition of early motor skills in the first year of life, followed by slowly progressive symptoms and cerebellar signs with loss of developmental landmarks [39]. These symptoms are primarily caused by a progressive decrease in myelination and white matter in the CNS, known as hypomyelinating leukodystrophy [38, 39]. The symptoms of SPAX8 are similar to those of other leukodystrophies, such as Pelizaeus-Merzbacher disease, Alexander disease and ARSACS, suggesting a possible connection between the molecular and cellular mechanisms of these disorders [41]. However, the correlation between SPAX8 genotype and phenotype is still barely understood [39]. NKX6-2 loss-of-function mutations have been linked to myelination defects in SPAX8 and other neurological and behavioral disorders [42, 43]. Additionally, hypermethylation of the NKX6-2 gene is linked to pathologies such as cancer [44] intellectual impairment and autism [45].

To date, 40 cases of SPAX8 in 24 families have been identified involving 18 mutations in the NKX6-2 gene worldwide: eight missense mutations, six nonsense mutations and four frameshift mutations [46, 47, 48, 49] (Table 1.1). The two most recent cases are two women

from different families, diagnosed at ages 6 and 17, with the nonsense mutation c.475C>T (p.Gln159*) and frameshift mutation c.234delG (p.Leu79CysfsX109), respectively. Symptoms of both were similar, and led scoliosis, central hypotonia, hyperreflexia, spastic quadriplegia, osteopenia, and bilateral hip dysplasia [48].

The disease progresses in accordance with the age of onset. As a result, the earlier the disease manifests, the faster it spreads [40, 41]. Each stage is distinguished by distinct symptoms that reflect the disease's onset. Individuals who develop the disease before the first year of life demonstrate a failure of age-appropriate head control skills (70% of cases) and verbal goals (90%). Clinically, the phenotype stabilizes after development and adolescence [46], but 12.1% of cases result in death before the age of five years [40]. Children who develop the disease after the first year of life usually present motor delays and become wheelchair-dependent 3 to 8 years later [40]. The disease worsens continuously until the age of 25, when it finally stabilizes, which appears to coincide with the brain's full maturation [46]. The oldest SPAX8 patient was 44 years old, although life expectancy is still unclear due to the disease's rarity [39, 46].

Table 1.1 Variant description of NKX6-2 mutations that cause SPAX8 [46, 47, 48, 49].

Type of mutation	cDNA change	Amino acid change
Missense	c.301C>A	p.Arg101Ser
	c.487C>G	p.Leu163Val
	c.501C>G	p.Phe167Leu
	c.541C>G	p.Leu181Val
	c.545C>T	p.Ala182Val
	c.592A>G	p.Asn198Asp
	c.598C>T	p.Arg200Trp
	c.599G>A	p.Arg200Gln
Nonsense	c.121A>T	p.Lys41*
	c.475C>T	p.Gln159*
	c.571C>T	p.Gln191*
	c.565G>T	p.Glu189*
	c.589C>T	p.Gln197*
	c.608G>A	p.Trp203*
Frameshift	c.196delC	p.Arg66Glyfs*122
	c.224dup	p.Leu79Alafs*?
	c.234delG	p.Leu79CysfsX109
	c.606delinsTA	p.Lys202Asnfs?1

1.2 The NKX family of transcriptional regulators

The NKX family includes four classes of transcriptional regulators known as NKX1, 2, 3, and 6. These classes give rise to 13 different NKX proteins, which typically function as transcriptional repressors to control the development of organs and cells [50]. The NKX family is distinguished by a conserved homeobox domain. The genes that they control and their biological functions are still barely understood. There is a higher degree of homology shared by members within the same class (30-50%) than by members of different classes (25%). NKX genes are expressed in numerous organs and tissues, and their patterns of expression frequently overlap [41].

The NKX1 class has two known members: NKX1-1 and NKX1-2. NKX1-1 is found on chromosome 4 and is linked to Wolf-Hirschhorn Syndrome [51, 52], which is characterized by ataxia, head abnormalities, and impairments in the heart, growth, and urinary system due to deletions in the short arm of this same chromosome. Energy homeostasis is also influenced by this gene in mice [53, 54]. NKX1-2 affects Wnt/β-catenin signaling, controls the development of mesendoderm, and promotes adipogenesis [52]. NKX2-1, NKX2-2, NKX2-3, NKX2-4, NKX2-5, NKX2-6, and NKX2-8 are the seven members of the second class. NKX2-1, also known as thyroid transcription factor-1 (TTF-1), is an oncogene linked to several forms of cancer and is a key regulator of gene transcription in the thyroid gland, lung and brain [55, 56]. NKX2-2 is required for V3 domain specification during neural tube patterning in the embryonic stage, as well as later oligodendrocyte maturation [57]. NKX2-3 and NKX2-4 are activated in acute myeloid leukemia, downregulating genes involved in megakaryocytic and erythroid differentiation processes, contributing to the development of disease subtypes [58]. NKX2-5 controls cardiac development [59], whereas NKX2-6 controls pharyngeal development [60]. NKX2-8 still has unspecified function, but recent evidence indicates that it represses the transcription of the multidrug resistance gene 1 (MDR1), indicating a correlation of NKX2-8 with drug sensitivity of urothelial carcinoma cells [61]. NKX3-1 and NKX3-2 are the only two members of the third class. NKX3-1 is a tumor suppressor in prostate carcinogenesis, responsible for regulating prostate development [62]; while NKX3-2 is a regulator of chondrocyte and distal stomatal cell development in collaboration with Bapx1 [63, 64].

Finally, the fourth class has three members: NKX6-1, NKX6-2, and NKX6-3. The determination and differentiation of neuronal populations and oligodendrocytes in the basal nuclei, ventral diencephalon, and mesencephalon during early development depends on the coordination between transcription factors NKX6-1 and NKX6-2 [65, 66, 67]. Additionally, the function, proliferation and differentiation of pancreatic cells are also significantly influenced by both NKX6-1 and NKX6-2 [64, 65]. The human NKX6-2 protein shares 97% identity with mouse NKX6-2 [68]. The NKX6 class have almost identical sequences: the only differences between the homeodomains of NKX6-1 and NKX6-2 are three conserved amino acid alterations. The C57BL murine models are affected by the loss of NKX6-2 function, as this impairs myelination and consequently the CNS nerve conduction and motor coordination [43]. An abnormal structure of myelin sheaths and more severe neurological effects are observed in the same NKX6-2-/- mouse models that also carry a heterozygous inactivating mutation in NKX2-2 [69]. Despite the sequence similarity of NKX6-1 and NKX6-2, there are

some critical differences. For example, NKX6-2 is not as expressed in humans in oligodendrocyte precursors as NKX6-1 [67] but is expressed in differentiated postmitotic oligodendrocytes [70]. Both play a different role in the formation of oligodendrocytes [71], while the lack of NKX6-2 causes paranodal defects in oligodendrocyte development [43]. This evidence, and the fact that loss-of-function mutations in both NKX6-2 alleles are sufficient to produce SPAX8, suggests that there is no redundancy between these NKX6-1 and NKX6-2 in humans, as opposed to what has been observed in mouse models [46]. Lastly, NKX6-3 inhibits metastasis and cancer cell migration and invasion caused by Wnt/β-catenin and Rho-GTPase; and the development of gastric cancer is directly influenced by the degree of NKX6-3 expression [72].

1.2.1 NKX6-2

NKX6-2 is found on chromosome 10q26.3, with 3 exons and 2 introns totaling 1033 nucleotides (Ensembl v109 data) [73]. It was initially identified in a mouse embryo cDNA library searching for homeobox proteins associated with tissue development. The gene, initially named as the glia- and testis-specific homeobox gene (Gtx), was identified in glial cells of adult mice and was later reported to be active in mouse embryonic glial cells [74]. Due to its similarity to other NKX family members, the gene was renamed NKX6-2.

Following translation, a protein with 277 amino acids (29 kDa) is formed, with a predominantly nuclear localization that has been experimentally confirmed just recently. The region between amino acids 89-142 possibly corresponds to the repressor domain, but the confidence score for these residues is still very low (data from Uniprot v2023) [75]. The protein's structure is still unknown, and the existing structure of the homeobox domain was only inferred computationally by homology with the crystal structures of the Aristaless and Clawless homeodomains using the Swiss model repository [76]. The complete structure was also computationally inferred by AlphaFold v2.0 [77] (AF-Q9C056-F1, *https://alphafold.ebi.ac.uk/entry/Q9C056*) (**Figure 1.5**).

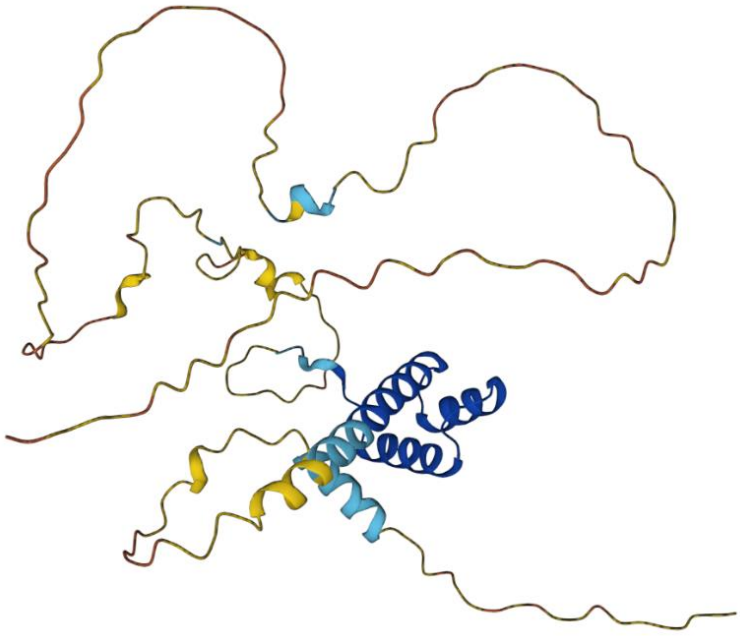

Figure 1.5 — Predicted structure of NKX6-2. Identifier: AF-Q9C056-F1 by AlphaFold v2.0 (2023).

In an extremely sequence-specific manner, the homeobox (amino acids 148-207), a highly conserved DNA binding domain, mediates precise interaction with the minor and major grooves of DNA and mediates transcription [77, 78, 79]. Genes with homeobox domains act as master genes, controlling positional information during embryonic development and pattern formation. They normally maintain the differentiated states of adult cell populations and direct the renewal of specific cell types. These homeobox genes have widespread expression in the development of vertebrate nervous system, but only a few, such as NKX6-2, remain active in adulthood [80]. The C-terminus (residues 208–277) of NKX6-2 may feature a transactivation domain (TAD), which was suggested by sequence homology with other family members and is deleted in most protein-truncating variations. High-throughput mass spectrometry has shown that this putative TAD can be acetylated (K215) and phosphorylated (Y238, S246 and T252) in rats (**Figure 1.6**). These analyses did not focus specifically on NKX6-2, and the function of TAD post-translational modifications is still unknown [81].

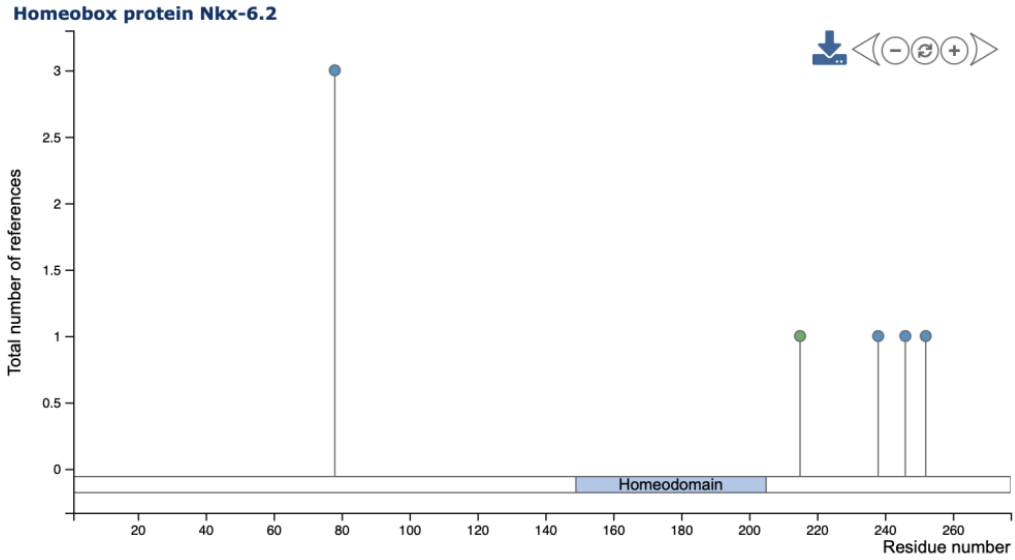

Figure 1.6 — Representation of NKX6-2 phosphorylation and acetylation sites. The G78 phosphorylation site (in blue) seen on the left is outside the transactivation domain. Then the acetylation site K215 (in green) and the phosphorylation sites Y238, S246 and T252 (in blue), respectively. Image retrieved from *www.phosphosite.org*.

A significant amount of NKX6-2 mRNA was found in the CNS, mostly in the spinal cord, and shows strong and long-lasting expression in oligodendrocytes until adulthood [43]. The stomach also shows high levels of NKX6-2 mRNA, according to transcriptomic analyses of human tissues that were made available in the Protein Atlas data-base [82]. Lower levels of NKX6-2 mRNA are found in the pancreas, testicles, esophagus, vagina, kidney, colon, and cardiac muscle [82]. At a cellular level, high expression was found in oligodendrocytes and gastric mucus-secreting cells, and lower expression levels in Schwann cells, spermatogonia germinative cells, and astrocytes. In cancer cells, it is highly concentrated in glioblastoma [83] and to a lesser extent in gastric and pancreatic cancer. However, NKX6-2 has frequent deletions in cerebral tumors [84].

NKX6-2 regulates myelin-related genes such as myelin basic protein (MBP) and proteolipid protein (PLP), in addition to genes involved in differentiation and development such as Dbx2 and Myt1 [62]. The NKX6-2 gene binds to the promoter regions of MBP and PLP1, which are directly related to the regulation of axon-glial interactions in myelin paranodes in oligodendrocytes (data from Uniprot v2023) [75]. The consensus DNA response element is 5'-(A/T)TTAATGA-3' usually exerting repressive effects on transcription [84].

1.2.2 NKX6-2 as a transcriptional repressor and regulator of motor neurons

Sonic hedgehog (Shh) is an extended morphogen responsible for the division of five distinct spatial domains called p0, p1, p2, pMN (progenitor of the motor neurons), and p3 [85]. The Shh pathway and NKX6-2 function are closely associated during embryonic development and, in conjunction with a contrasting gradient of the BMP/Wnt pathway, determine the dorsal-ventral axis in the CNS [86]. The proteins controlled by the Shh pathway are classified into two classes: Class I, where the constitutive expression of proteins is inhibited by Shh, and Class II, where the expression of proteins is activated by Shh [87]. A protein from Class I represses a protein from Class II, and vice-versa. During brain development, the interaction between NKX6-1 and NKX6-2 (Class II) and Dbx1 and Dbx2 (Class I) regulate the spatial patterning from p0 towards pMN. Shh morphogen levels then rise from the dorsal to the ventral area, increasing the expression of NKX6 genes and decreasing the expression of Dbx genes [88]. In a subsequent step, the four proteins inhibit one another's transcription, resulting in the development of four distinct cell populations that only express one of the proteins. These populations will differentiate into multiple types of neural progenitors (p0, p1, and p2). If NKX6-2 is absent, NKX6-1 can compensate by repressing the expression of Dbx1 [89]. Another combination might be NKX6-1 and Dbx2, which separate the p1 and p2 cells in neural tissue, and NKX6-1 can inhibit NKX6-2 during the transitions between these populations. In other words, NKX6-2 and NKX6-1 are initially co-expressed in a broad ventral domain, but their expression eventually becomes mutually exclusive, partly due to the repression of NKX6-2 by NKX6-1 [67, 68]. NKX2-2 (Class II) and Olig2 (Class I) transcriptional factors are additionally paired directly to generate a divide between pMN and p3 progenitor cells [88]. The four proteins define the different neural cell populations before coordinating the transition to motor neurons (MNs) and the V0-3 neural cell subtypes (**Figure 1.7**) [89, 90]. The pathway would later advance to the generation of astrocytes from p0-p3 progenitors and oligodendrocytes from pMN cells [69], with NKX6-2 engaged in oligodendrocyte maturation [91].

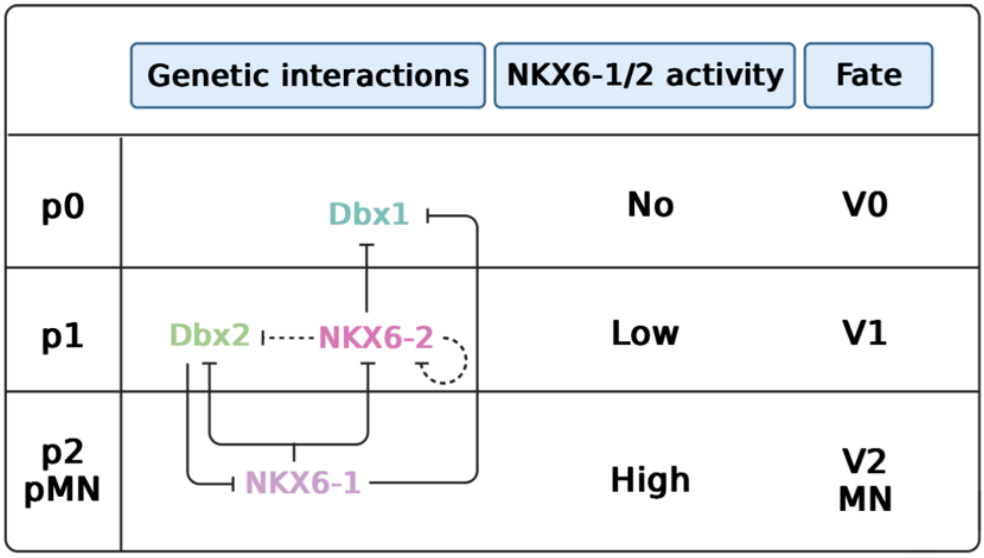

Figure 1.7 — p0, p1, p2, and pMN's neural cell fate is influenced by interactions between the NKX6 and Dbx transcription factors. NKX6-2/Dbx1, NKX6-1/Dbx2, and NKX6-1/NKX6-2 interact in the development of distinct cell populations. The four proteins cooperate genetically to determine the destiny of neural cells. Image adapted by A. Vallstedt, *et al*. (2001) [89] and created with *BioRender.com*.

Olig1/2 is required for the generation of all oligodendrocytes [92]. Oligodendrocytes originate from the ventral pMN domain as well as from dorsal progenitors. This phenomenon is attributed to the inhibition of Olig2-dependent cell specification, induced by elevated concentrations of bone morphogenic proteins (BMPs). Under normal circumstances, Olig2 expression is facilitated when BMP signaling is suppressed, so the gradual reduction in dorsal BMP signaling exerts an influence on the temporal emergence of oligodendrocytes within the dorsal neural tube through development [93].

Other transcription factors contribute to ventral neural patterning in collaboration with NKX6-1 and NKX6-2 [94, 95]. The proteins NKX6-1 and NKX6-2 are expressed in the ventral neural tube and are required for ventral Olig2 expression and the generation of MNs in the spinal cord. In mice lacking NKX6-1/2 proteins, ventral extinction of Olig2 expression possibly affects pMN-derived oligodendrocytes [88, 93]. NKX2-2 is both sufficient and necessary for the generation of V3 neurons in the spinal cord, and it is a confirmed repressor of Olig2 expression at this axial level [95]. Nevertheless, the differential regulation of oligodendrocytes by NKX6-1/2 proteins is strongly associated with NKX2-2 expression and the distinctive ventral origins of oligodendrocytes within the spinal cord and hindbrain [95]. Onecut Factors OC-1, OC-2 and OC-3 are also transcriptional regulators that influence MN diversification in the spinal cord [96, 97, 98]. Upregulation of NKX6-2 expression was observed in the

Oc1/Oc2$^{-/-}$ conditional knockouts (cdKO), while constitutive Oc1/Oc2$^{-/-}$ knockouts showed downregulation of NKX6-2 expression [96] **(Figure 1.8).**

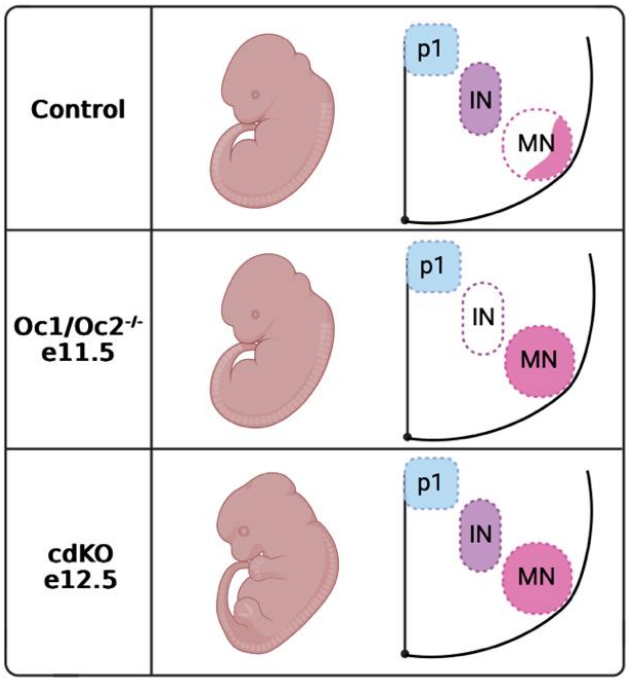

Figure 1.8 — NKX6-2 expression is up-regulated in conditional double mutant while it is down-regulated in the spinal cord of Oc1/Oc2$^{-/-}$ mutant embryos. The scheme represents an in situ hybridization for NKX6-2 at the lumbar, thoracic and brachial levels in control and constitutive Oc mutant (Oc1/Oc2$^{-/-}$) e11.5 and conditional double mutant (cdKO) e12.5. In control embryos, NKX6-2 was expressed in p1 progenitors and in ventral INs at all 3 levels (brachial, thoracic, and lumbar) and in some MNs at the lumbar and brachial levels. In the Oc1/Oc2$^{-/-}$ mutant, NKX6-2 continued to be expressed in p1 progenitors, was completely lost in ventral INs, and expanded in brachial and lumbar MNs. In cdKO, NKX6-2 expression remains in p1 progenitors, ventral INs and MNs. With this result, it is concluded that the negative regulation of NKX6-2 expression in the Oc1/Oc2$^{-/-}$ mutant is due to the elimination of expression in ventral INs despite expanding the MNs, while the positive regulation in the cdKO mutant is due to the expansion in MNs, without loss of ventral INs. Image adapted by M. Toch, *et al.* (2020) [96] and created with *BioRender.com*.

In summary, NKX6-2 acts as a transcriptional repressor and regulator of several genes ultimately necessary for motor functions, by promoting either the proper differentiation and distribution of specific types of neurons or the maturation and function of oligodendrocytes.

1.3 Regulation of the NKX family by phosphorylation

Among the more than 400 identified post-translational modifications (PTMs), phosphorylation, ubiquitination and acetylation are the most common and stand out as signal transducers. A PTM can be both reversible and irreversible. For example, covalent modifica-

tions (phosphorylation, acetylation, methylation, ubiquitination, etc.) are reversible reactions, whereas proteolytic cleavage are irreversible reactions [100]. Numerous protein behaviors and characteristics are impacted by these modifications, such as enzyme function and assembly [101], interactions between proteins [102], molecular trafficking [103], receptor activation [104], protein solubility, folding, localization or degradation/recycling [104, 105]. Phosphorylation can regulate the shuttle of transcription factors between the cytoplasm and the nucleus as well as their binding to DNA and activity, a role especially relevant in the context of this thesis. For example, STAT3 dimers phosphorylated at Y705 translocate to the nucleus and activate the transcription of genes involved in cell proliferation and survival [106]. Consequently, PTMs have a role in several biological processes, including signal transduction, gene expression regulation and activation, cell cycle control and DNA repair [100]. In this project, we focused on protein phosphorylation [107, 108]. For instance, the first phosphoprotein discovered was a metabolic enzyme called glycogen phosphorylase [109]. Phosphorylation occurs predominantly on Serine, Threonine and Tyrosine residues [110]. Kinases transfer a phosphate group from adenosine triphosphate, through a covalent attachment, to target residues. Conversely, different phosphatases catalyze protein dephosphorylation, that is, the removal of a phosphate group [111]. This mechanism is straightforward and adaptable, and ATP is readily available as a phosphoryl donor (**Figure 1.9**), and extremely common in eukaryotic organisms [109, 112]. Around 30% of the proteins encoded by the human genome are thought to include covalently bound phosphate, and aberrant phosphorylation is now understood to be a primary or secondary cause of a wide range of human disorders [113]. There are more than 250.000 phosphorylation sites throughout the proteome (*www.phosphosite.org)* in addition to more than 500 kinases [114] and more than 200 phosphatases [115] encoded by the human genome.

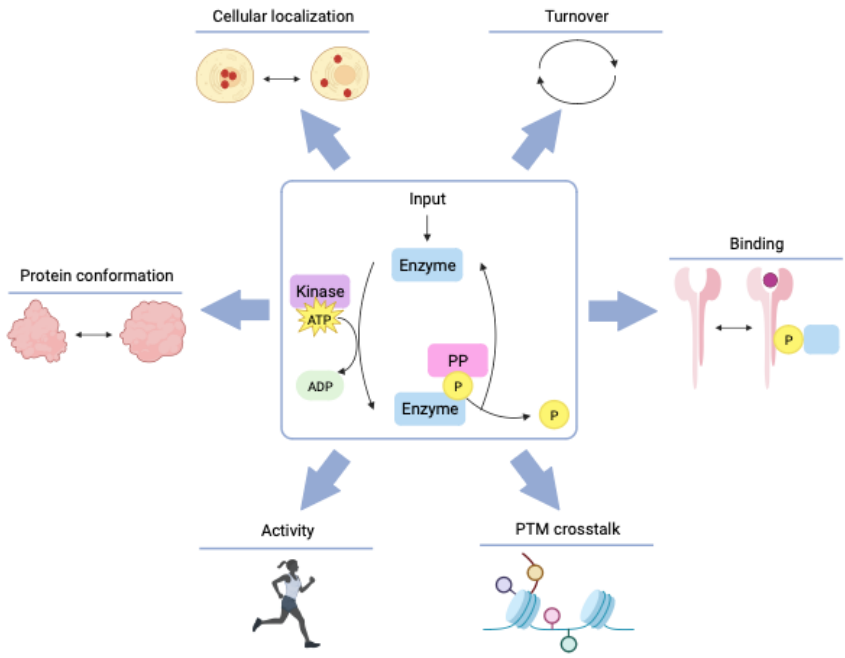

Figure 1.9 — Protein phosphorylation represents a molecular replacement mechanism. The addition of phosphate from ATP and the removal of phosphate from a phosphorylated protein substrate, which are both performed by enzymes called kinase protein and phosphatase (PP), respectively, are the two characteristics of reversible protein phosphorylation. This common post-translational modification (PTM) operates as a molecular replacement mechanism, regulating a variety of protein functions such as protein turnover, conformation, localization, interactions, enzymatic activity, and crosstalk with other PTMs, which in consequently control extensive cellular biological functions. Adapted image by Humphrey, S. J. (2015) [109] and created with *BioRender.com*.

The role of phosphorylation on the behavior and function of the NKX family is not so clear. NKX2-1 is phosphorylated on seven serine residues by a serine-threonine kinase. NKX2-1 transcriptional activation may require phosphorylation only in specific cell types [116]. The NK2-specific domain of NKX2-2 contains a potential Mitogen-activated Protein Kinase (MAPK) phosphorylation site, which plays a key role in the oligodendrocyte differentiation. The transcriptional activity of this protein can be regulated by phosphorylation of proteins through the specific domain of NK2 and modified by structural effects of specific sequences [117]. LIM Domain Kinase 2 (LIMK2) is a serine/threonine kinase that regulates cytoskeletal dynamics, is overexpressed in prostate cancer, and phosphorylates NKX3-1. NKX3-1 phosphorylation does not alter its subcellular localization but results in its proteasomal degradation. When overexpressed, LIMK2 modulates NKX3-1 expression at mRNA levels and decreases its stability [118]. NKX3-1 interacts with prostate-derived Ets factor (PDEF) and suppresses its ability to transactivate the prostate-specific antigen promoter. The high density and conservation of tyrosine residues in the C-terminal tail of NKX3-1 raises the possibility that perhaps this domain and the interaction between NKX3-1 and PDEF may be regulated by phosphorylation, as the ability to suppress PDEF transactivation in tumor cells

is interrupted if there is deletion of the C-terminal amino acids of NKX3-1 [119]. NKX6-1 presents six possible phosphorylation sites identified by high throughput mass spectrometry, whose influence and function are not yet known. On the other hand, NKX6-1 regulates Aurora Kinase A, causing its overexpression, which phosphorylates and degrades p53, removing this inhibitory factor and allowing the proliferation of β cells involved in type 1 and 2 diabetes [120]. NKX6-2 has four phosphorylation sites with yet unknown biological functions (see entry *www.phosphosite.org*), which are the focus of this thesis.

1.4 Objectives

The main objective of this work is to determine the possible influence of phosphorylation on the subcellular distribution of NKX6-2. To do this, we will create new NKX6-2 mammalian expression plasmids mutated at different described phosphorylation sites (S246, T252 and Y238) to mimic or inhibit phosphorylation. These plasmids will be transiently transfected into HeLa cells and tested by Immunoblotting and microscopy, so that both methods can serve as confirmation of each other regarding the expression, subcellular location and general behavior of the plasmids in living cells. This study provides new molecular tools for studying the regulation of NKX6-2 function in normal and pathological conditions.

2

MATERIALS AND METHODS

2.1 NKX6-2 Venus constructs

The pcDNA3.1-NKX6-2-Venus construct was synthesized by Invitrogen and deposited in the Addgene repository. The construct contains the sequence of the human NKX6-2 cDNA fused to the Venus fluorescent protein and optimized for mammalian expression, as well as ampicillin and neomycin selection cassettes. The single mutant constructs were produced by polymerase chain reaction (PCR)-based site-directed mutagenesis using the NKX6-2-Venus plasmid as a template. The double mutant construct S246A/T252A was produced by the same method but using the previously created single mutant NKX6-2-Venus S246A as DNA template. The original serine (S) on position 246 was replaced by alanine (A) or aspartic acid (D), the threonine (T) on position 252 was replaced by alanine (A) or aspartic acid (D) and the tyrosine (Y) on position 238 was replaced by phenylalanine (F) (**Figure 2.1**). Mutagenesis was performed using 20 ng of the plasmid template, 0,2 mM of deoxynucleotide triphosphates (dNTP) mix (NZYTech, Lisbon, Portugal), 0.2 µM of forward and reverse primers, and 2.5 U of PfuTurbo DNA Polymerase (Agilent Technologies, Santa Clara, CA, USA). The primers used for the mutagenesis were designed using PrimerX free software (*https://www.bioinformatics.org/primerx/*) (**Table 2.1**). The conditions were 2 min at 95º C and 30 cycles of 30 sec at 95º C, 7 min at 72º C (1 minute per kb) and 10 additional minutes at 72º C. The template DNA was digested with 10 U of Dpn I (NZYTech, Lisbon, Portugal) for 1 hour at 37º C, and the reaction was used to transform 25 µL of competent *Escherichia coli* cells (NZYtech, Lisbon, Portugal).

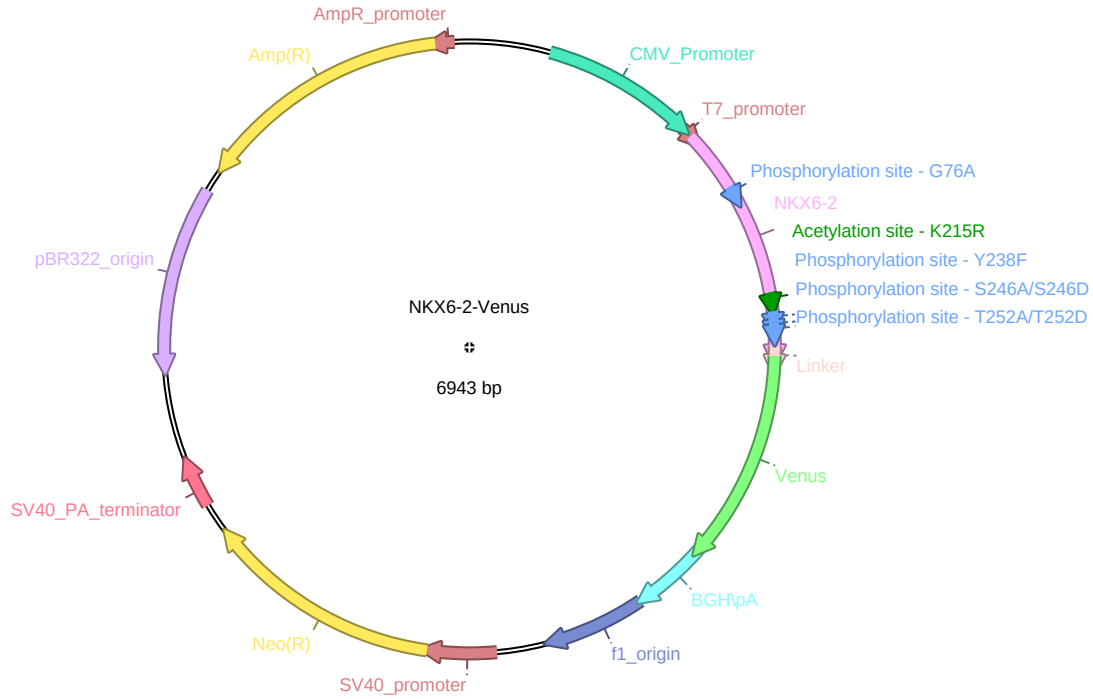

NKX6-2-Venus

GACACCATGGACACAAACAGACCTGGCGCCTTTGTGCTGTCTAGCGCTCCTCTGGCCGCTCTGCACAATATGGCCGAGATGAAGACCAGCCTGTTTCCAT
ACGCTCTGCAGGGACCTGCCGGCTTTAAGGCTCCTGCTCTTGGAGGACTGGGAGCACAACTGCCTCTGGGAACACCTCACGGCATCAGCGATATTCTGGG
CAGACCTGTTGGAGCTGCTGGCGGAGGATTGCTCGGAGGACTGCCTAGACTGAATGGACTGGCTTCTTCTGCCGGCGTGTACTTTGGACCTGCTGCTGCC
GTTGCCAGAGGCTATCCTAAACCTCTGGCTGAGCTTCCCGGCAGACCTCCTATTTTTTGGCCTGGTGTTGTGCAGGGCGCTCCTTGGAGAGATCCTAGAC
TTGCTGGACCAGCTCCTGCAGGCGGAGTGCTGGATAAGGATGGCAAGAAGAAGCACAGCAGACCCACCTTCAGCGGCCAGCAGATCTTTGCCCTGGAAAA
GACCTTCGAGCAGACCAAGTATCTGGCTGGCCCTGAGAGAGCCAGACTGGCCTATTCTCTGGGCATGACCGAGAGCCAAGTGAAAGTGTGGTTCCAGAAC
AGACGGACCAAGTGGCGGAAGAGACATGCCGTGGAAATGGCCAGCGCCAACAAGAAACAGGACAGCGACGCCGAGAAGCTGAAAGTTGGAGGCTCCGATG
CCGAGGACGACGACGAGTATAATAGACCTCTGGACCCCAACAGCGACGATGAGAAGATCACCCGGCTGCTGAAGAAACACAAGCCCAGCAATCTGGCCCT
GGTGTCTCCTTGTGGTGGCGGAGCTGGGGATGCACTTGGATCCGGCGGAGGTGGAAGCGGCGGAGGCGGATCTGGTACCATGGTTTCTAAGGGCGAAGAA
CTGTTCACCGGCGTGGTGCCTATCCTGGTGGAACTGGATGGGGATGTGAACGGCCACAAGTTCTCTGTGTCTGGCGAAGGCGAAGGGGATGCCACATACG
GCAAGCTGACCCTGAAGCTGATCTGCACCACAGGCAAACTGCCCGTGCCTTGGCCTACACTGGTCACAACACTCGGCTACGGCCTGCAGTGCTTTGCCAG
ATATCCCGACCACATGAAGCAGCACGATTTCTTCAAGAGCGCCATGCCTGAGGGCTACGTGCAAGAGCGGACCATCTTCTTCAAGGACGACGGCAACTAC
AAGACCAGGGCCGAAGTGAAGTTCGAGGGCGACACCCTGGTCAACAGAATCGAGCTGAAGGGCATCGACTTTAAAGAGGACGGCAACATCCTGGGCCACA
AGCTCGAGTACAACTACAACAGCCACAACGTGTACATCACCGCCGACAAGCAGAAGAACGGCATCAAGGCCAACTTCAAGATCCGGCACAACATCGAGGA
TGGCGGCGTGCAGCTGGCCGATCACTATCAGCAGAACACCCCTATCGGAGATGGCCCCGTCCTGCTGCCTGATAACCACTACCTGAGCTACCAGTCTGCC
CTGAGCAAGGACCCCAATGAGAAGAGGGATCACATGGTGCTGCTGGAATTCGTGACAGCCGCCGGAATCACACTCGGCATGGACGAGCTGTACAAATGAG

Figure 2.1 — pcDNA3.1 NKX6-2-Venus plasmid map. Sequence of NKX6-2 (Pink), linker (Light Pink) and Venus (Green). Phosphorylation sites location (G78, Y238, S246, T252, respectively) in blue and the acetylation site K215 in dark green.

Table 2.1 — Sequence of the primers used to perform PCR-based site-directed mutagenesis. Fwd: forward. Rev: reverse

Mutations	Primers
S246A	Fwd: 5' CTCTGGACCCCAACGCCGACGATGAGAAG 3'
	Rev: 5' CTTCTCATCGTCGGCGTTGGGGTCCAGAG 3'
S246D	Fwd: 5'CTCTGGACCCCAACGACGACGATGAGAAG 3'
	Rev: 5' CTTCTCATCGTCGTCGTTGGGGTCCAGAG 3'
T252A	Fwd: 5'ACGATGAGAAGATCGCCCGGCTGCTGAAG 3'
	Rev: 5' TTCAGCAGCCGGGCGATCTTCTCATCGTC 3'
T252D	Fwd: 5' GACGATGAGAAGATCGACCGGCTGCTGAAGAAAC 3'
	Rev: 5' TTTCTTCAGCAGCCGGTCGATCTTCTCATCGTCG 3'
Y238F	Fwd: 5' CGACGACGAGTTTAATAGACCTCTGGACC 3'
	Rev: 5' GGTCCAGAGGTCTATTAAACTCGTCGTCG 3'
S246A/T252A	Fwd: 5'ACGATGAGAAGATCGCCCGGCTGCTGAAG 3'
	Rev: 5' TTCAGCAGCCGGGCGATCTTCTCATCGTC 3'

2.2 Bacterial transformation and DNA purification

The mixture of DNA and competent cells was incubated at 4º C for 30 minutes, followed by a heat shock at 42 ºC for 45 seconds. Cells were then returned to 4º C for 2 additional minutes. Subsequently, 300 µL of Luria Broth (LB) medium (25 g/L of LB – NZYtech, Portugal) without antibiotics were added to the bacterial suspension and incubated at 37° C, in agitation (180 rpm) for 1 hour. Transformed bacteria were seeded on LB agar (40 g/L of LB Agar Miller – VWR Chemicals, USA) containing 100 µg/mL of ampicillin (AppliChem Panreac, Darmstadt, Germany) were used to seed the transformed bacteria and incubated overnight at 37º C. The colonies were poked the next day and cultured in 3 mL of LB medium containing 100 µg/mL of ampicillin overnight at 37º C in agitation (180 rpm). DNA was then extracted and purified using the ZR Plasmid MiniprepTM-Classic D4016 (Zymo Research, Irvine, CA, USA), following manufacturer's instructions. Finally, DNA was quantified by means of a Nanodrop 1000 (Thermo Fisher Scientific, Waltham, MA, USA) before it was submitted to STAB VIDA for sequencing (Caparica, Portugal). These constructs were later deposited In the Addgene public repository, and they will be available upon publication of these results.

2.3 Cell culture

HeLa (Clontech, USA) and 10B1 cells were maintained in Dulbecco's Modified Eagle Medium (DMEM) Low Glucose (1 g/l) with stable Glutamine (862 mg/L) and Sodium Pyruvate (110 mg/L) (biowest, Nuaillé, France), supplemented with 9% of pannexin (PAN-Biotech GmbH, Aidenbach, Germany), 1% of fetal bovine serum (FBS) (Sigma-Aldrich , St. Louis, USA) and 1% of a penicillin/streptomycin commercial antibiotic mixture (Thermo Fisher Cientific, Waltham, USA) at 37° C in a humidified environment containing 5% CO_2. The HMC3, C6 (Sigma-Aldrich, St. Louis, USA), $C6^{Sacs-/-}$ (previously described in [121]) and another 10B1 cells plate were maintained under the same conditions but the medium was supplemented only with 10% FBS and 1% penicillin/streptomycin commercial antibiotic mixture. Human 10B1 neural precursor cell line and HMC3 microglial cell line were kindly provided by Dr. Adelaide Fernandes (Faculty of Pharmacy, University of Lisbon). Medium was changed every other day and cells were passed once a week, when confluence reached 80%, using 3 mL of Trypsin (TrypLE Express, Thermo Fisher Scientific, Waltham, MA, USA) for 5 minutes at 37º C. After adding 7 mL of medium with serum to inactivate trypsin, the cell suspension was centrifuged at 500 x g for 5 minutes at room temperature. Cells were seeded for maintenance in a new 100 mm plate at 1:40 dilution after the pellet was resuspended in 5 mL of fresh media. Cells were counted using a Neubauer Chamber (Glaswarenfabrik Karl Hecht, Sondheim vor der Rhön, Germany) and seeded at a density of $4.8*10^4$ cells/cm^2 in different types of plates according to the type of assay. Cell transfection was performed 24 hours after seeding, using the jetPRIME reagent (Polyplus-transfection, USA) at a 1:3 proportion (1 µg of DNA: 3 µL jetPRIME), following the manufacturer's recommendations.

2.4 Microscopy

For microscopy experiments, cells were seeded and transfected in 35 mm glass-bottom dishes. Widefield fluorescent microscopy images were acquired using a Leica DMI6000B (Leica microsystems, Germany) equipped with a camera Monochrome CMOS 4.0 MP (2048 x 2048 pixels), and a 40x water objective. Image acquisition was carried out by means of the Las X software (Leica microsystems, Germany). Just prior to observation, nuclei were counterstained with Hoechst 33342 [0.6 ng/µl (Thermo Fisher, Waltham, USA)] for 5

minutes, and the excess was washed off with PBS (Thermo Fisher Scientific, Waltham, USA). Hoechst 33342 was observed using a filter cube that enables excitation at 330-385nm, with maximum emission at 461 nm, and Venus was observed using a filter cube that enables excitation at 450-490nm, with maximum emission at 528 nm. Microscopy images were analyzed for area, perimeter, circularity, solidity and average fluorescence using the "Analyze particles" function in Fiji ImageJ [122].

2.5 Protein extraction

For total protein extraction, 100mm plates were seeded with 10B1, HMC3, C6 and $C6^{Sacs-/-}$ cells. Cells were washed with 1x PBS and received 200 µL of lysis buffer (50mM Tris HCl, 150 mM NaCl, 1% NP-40, 1x protease inhibitor, 1x phosphatase inhibitor). Then the cells were transferred to centrifuge microtubes, sonicated (Fisher Scientific, Waltham, MA, USA) for 10 seconds and incubated on ice for 45 minutes. Finally, cells were centrifuged at 10,000 x g, 15 minutes at 4° C. The supernatant containing the total proteins was collected into new tubes and stored at -80° C until use.

Cells were seeded in 60 mm dishes for nuclear and cytoplasmatic protein extraction. Twenty four hours after transfection, cells were washed and collected into a microcentrifuge tube with 1 mL of PBS. Cells were then centrifuged at 500 x g for 5 min at 4° C. After this step, cells were incubated with 300 µL of cytosolic extraction buffer (milliQ H_2O, 50 mM HEPES, 2 mM EDTA, 10mM NaCl, 250mM Sucrose, 2 mM DTT, 0.1% NP40) at 4° C for 5 minutes and then centrifuged at 3000 x g for 4 minutes. The supernatant (cytosolic extracts) was collected into new tubes. An additional 150 µL of cytosolic buffer was added to wash the pellet, centrifuged again under the same conditions and the supernatant discarded. Next, the pellets were incubated with 100 µL of nuclear extraction buffer (milliQ H_2O, 50 mM HEPES, 2 mM EDTA, 400 mM NaCl, 20% Glycerol, 2 mM DTT) at 4° C for 20 minutes, shaking occasionally with the aid of the vortex every 5 minutes for approximately 10 seconds. A commercial protease inhibitor cocktail (Abcam, Cambridge, United Kingdom) was added to both buffers. Finally, the tubes were centrifuged at 10 000 x g for 10 minutes and the supernatant (nuclear extracts) collected into new tubes. Protein concentrations were quantified using the Bradford assay [123]. A standard curve with known concentrations of Bovine Serum Albumin [BSA, 0.125 to 2 µg/µL (G-Biosciences, USA)] was used to determine protein concentration. Samples were incubated with 200 µL of Bradford reagent (AppliChem Panreac, USA)

for 10 minutes and absorbance was measured at 595 nm in a Victor 3v microplate reader (Perkin-Elmer, USA).

2.6 Western Blotting

After protein quantification, 30 μg of total, cytoplasmatic and nuclear extracts were mixed with 1x loading buffer (25% of Tris-HCl pH 6.8, 10% sodium dodecyl sulphate (SDS), 25% glycerol, 20% β-mercaptoethanol, 0.008% bromophenol blue), incubated at 95º C for 5 minutes and at 4º C for 5 minutes. Samples were separated by SDS-PAGE in 4% v/v SDS-acrylamide stacking gel electrophoresis and 10% v/v SDS-acrylamide stacking gel, at 120V for 80 minutes in running buffer (25 mM Tris, 190 mM glycine, 0.1% SDS). The protein molecular marker used was the NZYColor Protein Marker II (Lisbon, Portugal). Proteins were transferred to a nitro-cellulose membrane (Bio-rad, USA) at 100V for 1 hour in transfer buffer (25 mM Tris, 190 mM glycine, 20% methanol). The efficiency of sample transfer was confirmed by Ponceau S staining [1.4 mM Ponceau S (Amresco, Solon, OH, USA), 5% acetic acid]. Membranes were washed with Tris-Buffered Saline with Tween 20 (TBS-T) (TBS 1x, 0,05% Tween-20) on a bench rocker 25 (Labnet, USA) at 80 rpm. Membranes were blocked for 1 hour at room temperature with 5% non-fat dry milk in TBS-T. After that, they were washed three times for 10 minutes each in TBS-T and then incubated overnight at 4º C with the primary antibodies (**Table 2.2**), which were diluted in 5% BSA, 0.05% sodium azide and TBS-T. Next day, membranes were washed three times for 10 minutes and incubated for 2 hours at room temperature with the appropriate secondary antibodies (**Table 2.3**), which were diluted in 5% non-fat dry milk in TBS-T. Then, membranes were washed again for 10 minutes each and incubated for 1 minute with Peroxidase and Luminol Solutions from PierceTM ECL Western Blotting Substrate (Thermo Fisher Scientific, USA), and chemiluminescence was recorded in an Amersham Imager 680 RGB (Cytiva, Marlborough, MA, USA).

Table 2.2 — Primary antibodies used in this project.

Primary antibody	Dilution	Manufacturer	Reference
Anti-NKX6-2 (rabbit)	1:1000	Invitrogen, USA	PA5-48988
Anti-GAPDH (mouse)	1:1000	Santa Cruz Biotechnology, Dallas, USA	sc-32233
Anti-PCNA (mouse)	1:500	Santa Cruz Biotechnology, Dallas, USA	sc-56

Table 2.3 — Secondary antibodies used in this project.

Secondary antibody	Dilution	Manufacturer	Reference
Goat anti-Rabbit IgG (H+L)	1:10000	Thermo Fisher Scientific, Waltham, MA, USA	A16096
Goat anti-Mouse IgG (H+L)	1:10000	Thermo Fisher Scientific, Waltham, MA, USA	A16066

2.7 Statistical Analysis

Data were presented as the mean of at least 3 independent experiments ± standard error (SEM). Statistical comparison between two groups was performed using the unpaired t-test with Welch's correction and experiments involving more than two groups were analyzed by means of one-way ANOVA test followed by the Dunnett's post hoc test. All statistical analyzes were performed with GraphPad Prism 9 (GraphPad Software Inc., San Diego, CA, USA). P values lower than 0.05 were considered statistically significant (*P < 0.05; **P < 0.01; ***P < 0.001; ****P <0.0001).

3

RESULTS

3.1 NKX6-2 locates to the nucleus in a phosphorylation-independent manner.

We developed six NKX6-2 mutants to inhibit (S246A, T252A, S246A/T252A and Y238F) or mimic (S246D and T252D) phosphorylation. Wild-type (WT) NKX6-2 protein showed exclusively nuclear localization as determined by both microscopy and western blotting (**Figure 3.1**). No mutant altered the subcellular distribution of the protein. Despite this, most of these mutations affecting the TAD domain considerably increased protein levels compared to WT, as determined by both microscopy (**Figure 3.1 A and B**) and immunoblotting (**Figure 3.1 C and D**) approaches. The phosphomimic S246D showed significant increases in NKX6-2-Venus levels by both microscopy and immunblotting, while the corresponding phosphoresistant mutant S246A was the one that showed expression levels more similar to the WT. The T252 mutants showed a strong tendency to higher protein levels, but it only achieved significance in microscopy analysis (**Figure 3.1 A and B**). The SA/TA double mutant shows levels of expression between S246A and T252A single mutants (**Figure 3.1**). The Y238F mutant significantly increased the concentration of the NKX6-2 protein, presenting the highest protein levels in both microscopy and immunoblotting experiments (**Figure 3.1**).

The fact that the S246A phosphoresistant mutation demonstrates lower mean fluorescence than the corresponding phosphomimic mutation indicates that NKX6-2 phosphorylation in this residue could control protein stability or degradation. On the other hand, while the T252A phosphoresistant mutation slightly increases fluorescence compared to the T252D phosphomimic mutation, it does not present significant difference, suggesting that the phosphorylation of this residue is not directly involved in NKX6-2 stability or degradation. However, it cannot be ruled out that the alteration of this residue induces phosphorylation at S246

or other structural changes that can influence indirectly the stability of NKX6-2. The results of this study can also be partially seen in [81].

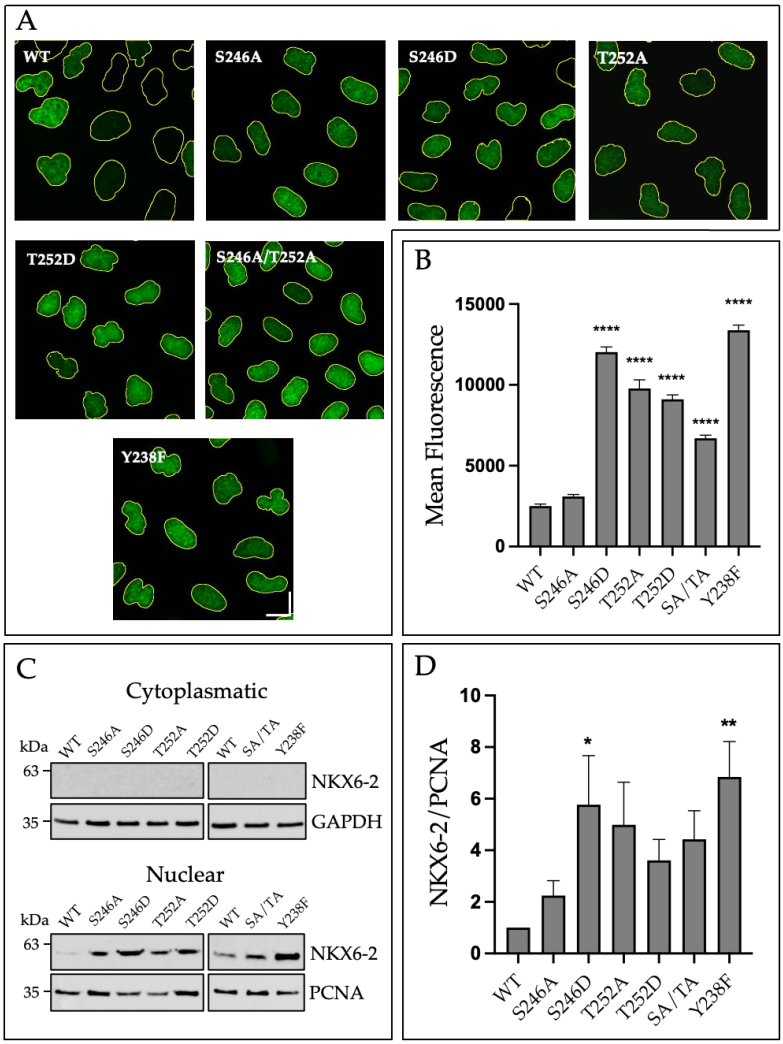

Figure 3.1 — Nuclear expression of NKX6-2-Venus mutants in HeLa cells. Nuclear expression of NKX6-2-Venus mutants in HeLa cells. A) HeLa cells transfected with NKX6-2-Venus (WT) and NKX6-2-Venus mutants (green) that inhibit (S246A, T252A, S246A/T252A and Y238F) and mimic (S246D and T252D) phosphorylation. The nuclei were stained with Hoechst and outlined in the images (yellow). Images processed by imageJ. Scale bar = 20 µm. B) Graphical representation of the mean fluorescence of all mutants compared to WT. Only the S246A mutant does not show a significant difference. The data was obtained using the "Analyze particles" function in imageJ, processed in Excel and formatted into a graph using GraphPad. Mean fluorescence was measured in n=4 independent experiments of each construct, counting in total WT: 365 cells, S246A: 333 cells, T252A: 347 cells and SA/TA: 384 cells. C) NKX6-2-Venus with the mutations of interest (57kDa) was detected in Western Blots only in the nuclear extract using an anti-NKX6-2 antibody. The loading control of the cytoplasmic and nuclear extracts was carried out using GAPDH (36 kDa) and PCNA (35 kDa), respectively. D) Quantification of NKX6-2 immunoblot bands of nuclear protein extracts from HeLa cells transfected with 1µg of DNA. Results were normalized with respect to PCNA levels and with respect to the control group in each experiment. Optical band densities were measured in n = 9 independent experiments for the WT and T252D mutant, n = 5 for the Y238F mutant, and n = 7 for the remainder of the constructs. The statistical analysis used in both graphs was One Way ANOVA followed by Dunnett's post hoc test and presented as mean ± SEM. Asterisks indicate significance versus WT: *, $p<0.05$; **, $p<0.01$, ****, $p<0.0001$.

3.2 NKX6-2-Venus mutants cause abnormal nuclear morphologies

Previous studies from our lab suggested that NKX6-2-Venus caused an abnormal shape in cells that overexpressed it, compared to cells lacking the transgene [124]. The nuclei of the human cervical cancer cell line HeLa are already known to have abnormal ellipsoids, ridged or notched nuclear shapes [125]. However, cells transfected with NKX6-2-Venus Wild-type tended to increase the percentage of abnormal nuclei from 51% to 64% (**Figure 3.2**). The T252D mutant further increased the percentage of abnormal nuclei to 77%, being the mutation in which this event is most observed. The T252A, SA/TA and Y238F mutants also increased the percentage compared to the nuclei without transfection but had similar results to the NKX6-2-Venus Wild-type. The S246A and S246D mutants remained at similar levels to untransfected nuclei. The nuclear abnormality may be related to the increased concentration of proteins, as in some mutants with a high percentage of abnormal nuclei, there are high levels of Venus fluorescence, that is, a higher concentration of proteins.

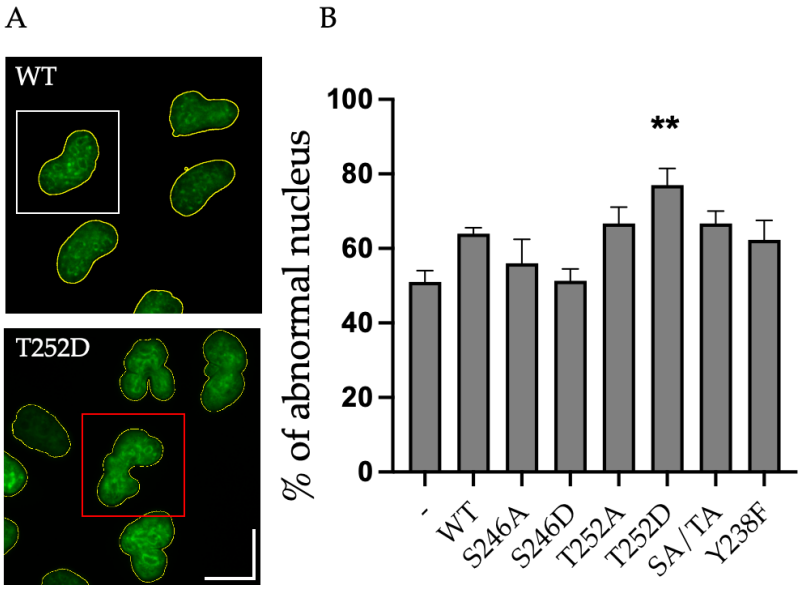

Figure 3.2 — The NKX6-2-Venus-T252D mutation increases the percentage of abnormal nuclei. A) Microscopy image of living HeLa cells transfected with NKX6-2-Venus. Normal nucleus transfected with NKX6-2-Venus (WT) represented in white box and abnormal nucleus transfected with the T252D mutant, represented in red box. B) The percentage of abnormal nuclei increases from untransfected (-) nuclei to nuclei transfected with the protein in its wild-type (WT) form. The studied S246 mutations do not considerably increase the number of abnormal nuclei, unlike T252 mutations, especially T252D. SA/TA and Y238F increases the amount similarly to WT. Compared to nuclei without tranfection, the T252D mutant shows a significant increase in abnormal nuclei (** $p<0.01$). The data was analysed in n=4 and presented as mean ± SEM and analyzed using One Way ANOVA followed by Dunnett's post hoc test. Scale bar = 20 µm.

A quantitative morphological analysis was performed based on microscopic experiments, comparing the mutants with WT NKX6-2 (**Figure 3.3**). Regarding the area of the nuclei, the Y238F mutant demonstrated a significant increase, indicating larger than normal nuclei. This result could be related to the increase in protein levels of this mutant (**Figure 3.1**). The perimeter was similar in most mutations, except for the SA/TA mutants, which showed a slight but significant increase. The circularity of the nuclei appears to be affected in the T252A and SA/TA mutants, decreasing considerably. This decrease in the circularity of these mutants may be related to the slight, non-significant increase in the percentage of abnormal nuclei (**Figure 3.2**). The analysis of the solidity of the nuclei shows practically identical levels in all mutants.

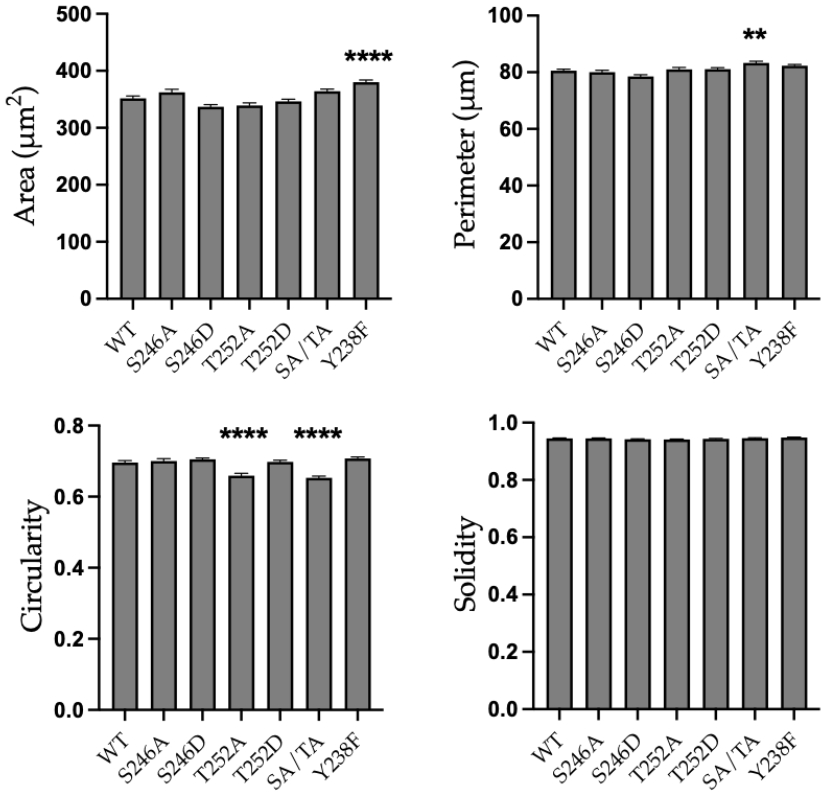

Figure 3.3 — The Y238F mutant has relatively larger nuclei, while SA/TA mutant demonstrates increased perimeter and less circular nuclei, along with T252A. Y238F was the only mutant to demonstrate a significant increase in area. The levels observed regarding the perimeter showed little difference, with a significant increase in SA/TA. The circularity analysis demonstrates that the T252A and SA/TA mutants obtained a decrease in this parameter and the solidity shows similar levels in all mutants. The data were obtained using the "Analyze particles" function in imageJ, processed in Excel and formatted into graphs using GraphPad. The different parameters were measured in n=4 independent experiments of each construct, counting in total WT: 365 cells, S246A: 333 cells, S246D: 372 cells, T252A: 347 cells, T252D: 369 cells, SA/TA: 384 cells and Y238F: 402 cells. Data are presented as mean ± SEM and analyzed using One Way ANOVA followed by Dunnett's post hoc test, asterisks indicate significance versus WT and the results were considered significant when the P value <0.05 (**<0.01; ****<0.0001).

3.3 NKX6-2 endogenous expression

Next, with the intention of developing a knockout cell model for NKX6-2, endogenous expression of the protein was tested in 5 cell lines (HeLa, 10B1, HMC3, C6 and C6$^{Sacs-/-}$). The five strains tested showed bands at 29 KDa, compatible with the size of NKX6-2 (**Figure 3.4**).

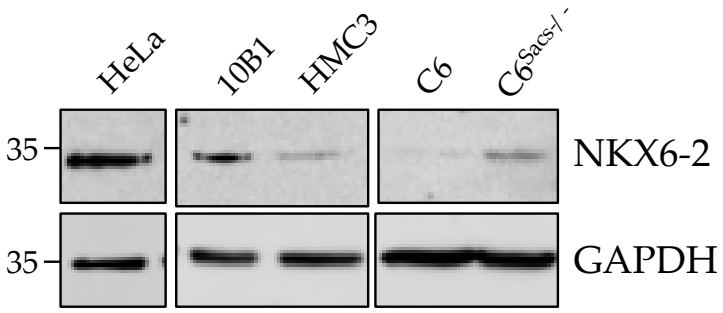

Figure 3.4 — Five cell lines express endogenous NKX6-2. HeLa cells without transfection show expression of endogenous NKX6-2 (29kDa), 10B1 and HMC3 glial cells also express endogenous NKX6-2 in agreement with these results. Finally, mouse C6 cells apparently show a weak expression signal, unlike C6$^{Sacs-/-}$ cells, which demonstrate greater expression of the NKX6-2 protein. Charge control of the extracts was performed by GAPDH (36 kDa).

The 10B1 cells are a line of human glial precursor cells that express markers of immature glial cells [126] and may be useful for studying the role of precursor cells in SPAX8 and other ataxias. As we had already seen that they expressed NKX6-2 (**Figure 3.4**), we decided to analyze whether they also expressed other proteins involved in ataxias, neurodegeneration and neuroinflammation (**Figure 3.5**). 10B1 cells were cultured and maintained in two different ways: in culture medium with 10% FBS and in culture medium with 9% PAN + 1% FBS. This second option would be a possibility to almost replace FBS completely with a synthetic serum. Surprisingly, 10B1 cells did not express Nestin and S100B, typical of astroglia, regardless of culture conditions. However, they expressed the ataxia-related chaperone Sacsin and the transcription factor STAT3, both of which are relevant to neuroinflammatory and neurodevelopmental processes. Glial fibrillary acidic protein (GFAP) is a type III intermediate filament expressed by several CNS cell lineages, including astrocytes [82]. In 10B1 we observed its expression, although it also presents some non-specific bands, probably associated with the dilution of the primary antibody. Vimentin is also an intermediate filament that helps in the composition of the cytoskeleton, is expressed in a large part of mesenchymal cells (data from Uniprot v2023) [75], overexpressed in carcinomas and possibly involved in

tumor metastases. It shows slight expression only in 10B1 cells cultured and maintained in 10% FBS, indicating a low literal expression in these cells, however, when cultured in 9% PAN + 1% FBS medium, they did not grow and multiply sufficiently, thus causing a decrease in protein that may not even be detectable.

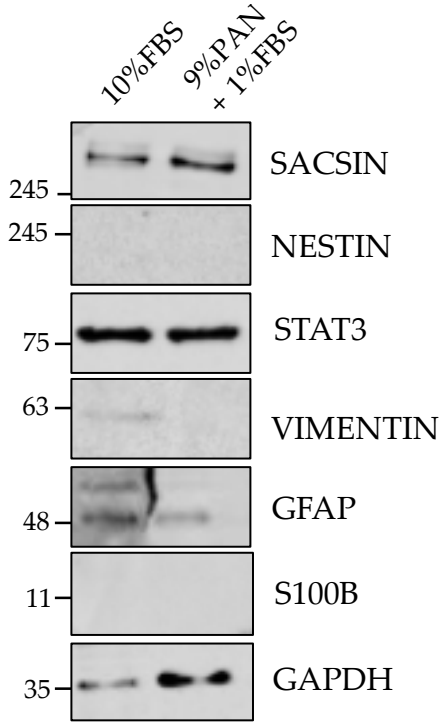

Figure 3.5 — Sacsin, STAT3, Vimentin and GFAP are expressed in 10B1 cells. Several proteins were detected by Wester Blots from total protein extracts. In cells cultured and maintained at 10%FBS, the proteins Sacsin, STAT3, Vimentin and GFAP were detected, while in cells cultured and maintained at 9%PAN + 1%FBS, GFAP expression was not observed. Nestin and S100B were not de-tected. Charge control of the extracts was performed by GAPDH (36 kDa).

4

DISCUSSION

Practically all members of the NKX family have phosphorylation sites, except NKX1-1 and NKX2-8. However, their function and biological activity remain poorly understood. To investigate the effect of phosphorylation on NKX6-2 biology, point mutants were developed to mimic or inhibit phosphorylation at the described sites. As phosphorylation can alter the subcellular localization of proteins [109], the initial focus was to observe the influence of phosphorylation on NKX6-2 trafficking. All NKX6-2 PTM mutants, as well as the wild-type protein (WT), showed exclusive nuclear localization, which suggests that the mutations do not affect the ability of the protein to enter or remain in the nucleus.

NKX6-2-Venus is located in the nucleus in the phosphorylated and dephosphorylated mutants S246 and T252, closest to the C-terminus part of the protein (**Figures 3.1 A and C**). The S246A mutation showed less fluorescence than the other mutants (**Figure 3.1 B**), was always less detected in the immunoblot bands (**Figure 3.1 C and D**) and thus obtaining greater similarity with the WT. Of all the mutants studied, the S246A mutant is the one that most resembles the NKX6-2 WT, both in mean fluorescence (**Figure 3.1 A and B**), expression (**Figure 3.1 C and D**), abnormality of the nuclei (**Figure 3.2**), area, perimeter and circularity (**Figure 3.3**) indicating that the inhibition of phosphorylation at this site does not have a great influence on the behavior of the protein. The fact that the phosphomimic counterpart S246D alters the mean fluorescence and expression levels indicates that phosphorylation of this residue may be fundamental in the stability and/or degradation of NKX6-2. The specification of MNs is promoted by the phosphorylation of a Serine residue in the transcription factor Olig2, while dephosphorylation of this same residue later in development imbalances oligodendrocyte production [127]. As NKX6-2 is directly involved with Olig2 to generate a di-

vision between pMN and p3 progenitor cells [88], it is possible that its phosphorylation and dephosphorylation at this residue also influences this process.

The T252A and T252D mutants have a tendency towards higher levels of protein in terms of immunoblot bands (**Figure 3.1 C and D**) but it only achieves significance in fluorescence microscopy experiments (**Figure 3.1 B**). On the other hand, only the abnormality of the T252D nuclei is significantly different between them (**Figure 3.2**). The phosphorylation of a threonine at the C-terminus of phosphoprotein phosphatase-1 (PP1) has been associated with an inhibitory effect of this protein, so the control of phosphatase activity is also regulated by PTMs, which can result in various neuronal defects and the interruption of the cell cycle. It is important to note that PP1 is responsible for catalyzing a variety of phospho-serine (pS) and phospho-threonine (pT) dephosphorylation reactions in eukaryotes [128]. The differences observed between phosphomimic (S246D and T252D) and phosphoresistant (S246A and T252A) mutants in terms of protein expression give us the idea that phosphorylation can modulate the stability of NKX6-2.

We developed the SA/TA phosphoresistant double mutant to observe the behavior of the absence of phosphorylation in a mutant composed of two mutations already studied and analyzed separately, in which opposite effects on NKX6-2 protein levels had already been observed. The double mutant showed an expression level that was between the two solo mutants (**Figure 3.1**). This result suggests complex interactions within the TAD, with the possibility that multiple phosphorylation sites are involved in the regulation of NKX6-2 expression [129]. The Y238F mutant served to analyze the same hypothesis of repressive influence caused by the absence of phosphorylation, but in a region earlier than those we had already analyzed and a little closer to the homeobox domain. This mutant maintains the subcellular localization of protein in the nucleus and showed the highest increase in protein expression among the studied mutants (**Figure 3.1**). This clear increase observed only in this mutant may be related to the increase in nuclear area (**Figure 3.3**) or vice versa, as higher proteins tend to exceed the limits of the nuclei. On the other hand, the significant increase in protein concentration in the Y238F mutant (**Figure 3.1**) may indicate a unique role for this specific residue in regulating the stability or activity of NKX6-2.

As previously stated, the percentage of abnormal nuclei may be related to the increased concentration of the NKX6-2 protein. The S246D mutation contradicts this observation, as it increases the levels of protein expression observed through the immunoblot bands analyzed (**Figure 3.1 C and D**) but does not influence the shape of the nuclei compared to the

non-transfected nuclei (**Figure 3.2**). This can be explained through a thorough analysis of all the microscopic images obtained, in which we observed that protein expression was clearly higher in nuclei that had a different shape, although this mutation did not significantly increase the percentage of abnormal nuclei. In some specific locations in the nuclei, especially abnormal ones, a slightly higher concentration of the protein is noted, possibly causing a more visible immunoblot band to be detected. Another contradiction of this hypothesis is highlighted by Y238F, which demonstrates very high levels of mean fluorescence (**Figure 3.1 B**) and nuclear expression (**Figure 3.1 C and D**) but is not the mutation with the highest percentage of abnormal nuclei (**Figure 3.2**). Analyzing all the microscopy images obtained, we can notice that the cells transfected with Y238F presented abnormal nuclei always with high protein expression, while many more circular nuclei were also observed, these with lower protein expression. These data give us the idea that there are not so many abnormal nuclei, but those that are present have a very high concentration of the NKX6-2 protein, increasing the levels of media fluorescence and detection by immunoblot bands. Although this analysis slightly helps us in understanding the data, the possible relationship between a potential overexpression of NKX6-2 and nuclear morphology remains intriguing and further studies are needed to elucidate the underlying mechanisms and potential consequences of these nuclear anomalies, so that a conclusive result can be obtained.

We have shown that other point mutations associated with SPAX8 could result in NKX6-2 aggregation, some of them also close to the TAD. For example, R200W and L163V are examples of mutations in the NKX6-2 protein that cause exclusively nuclear aggregates [81]. Our PTM mutants do not produce protein aggregates, only greater protein concentration in small specific points of the nuclei, but if it was the case of a protein with a propensity to form aggregates, these aggregates would probably be more concentrated due to their exclusively nuclear location, which would force the protein to focus only on this space and not on the entire cell [81].

Hela cells showed endogenous NKX6-2 signal, although at lower levels than the exogenous NKX6-2 constructs. The behavior of our constructs should be analyzed in future projects in the context of HeLa knocked out for NKX6-2, to ensure that endogenous NKX6-2 does not interfere with the results. However, we have studied the behavior of several SPAX8-related mutants and each of them had specific features. The detection of endogenous NKX6-2 expression in several cell lines, including HeLa, highlights the potential relevance of NKX6-2 in different cell types (**Figure 3.4**). The expression of NKX6-2 in HeLa and 10B1 cells

is intriguing and may indicate a previously unreported role for NKX6-2 in these cells. The absence of typical astroglial markers (Nestin and S100B) in 10B1 cells, together with the expression of Sacsin and STAT3 (**Figure 3.5**), raises questions about the cellular identity of these cells. This observation suggests that 10B1 cells may have a unique phenotype or differentiation state that still requires further characterization. The expression of GFAP and Vimentin in 10B1 cells (**Figure 3.5**) may reflect their mesenchymal characteristics. The various expression patterns under different culture conditions should be further explored to better understand the factors that influence these intermediate filaments in these cells, as intermediate filaments are normally important players in regulating the physiological properties of cells, influencing cell motility and transduction signal [130].

All these results point to the complexity of the potential regulation of NKX6-2 by PTMs and highlight the need for additional studies to understand the mechanisms underlying our observations and the potential impact of this protein on cellular and pathological processes. The phosphorylation sites of NKX6-2 have not been discovered in humans, but they have the same conserved residues, so it is assumed that they can also be phosphorylated. An alternative way of analyzing NKX6-2 PTMs would be to combine immunoprecipitation assays of this protein, whether exogenous or endogenous, with mass spectrometry focused on the PTMs.

In the future, it would be interesting to develop the doubly phosphorylated SD/TD mutant to get a full idea of the effect of double phosphorylation and dephosphorylation. According to what was observed in the S246D and T252D single mutants, we can suggest that a doubly phosphorylated mutant maintains the level of expression between the levels that were observed in the single mutants, as one is slightly more expressed than the other, just as we found with the SA/TA dephosphorylated double mutant. However, as the T252D mutant has the highest percentage of abnormal nuclei, we can also assume that a double mutant will increase this percentage even more and, consequently, the level of expression. SA/YF and TA/YF are other phosphoresistant double mutants that would probably yield important information. We can assume that the SA/YF mutant would slightly increase the expression level compared to the simple S246A mutant, since it has low protein detection, while a greater increase in the expression level would be expected in TA/YF, due to the strength of expression already observed in T252A and mainly in Y238F. In this line of phosphoresistant mutants, it would also be interesting to develop a triple dephosphorylated SA/TA/YF mutant, which would hypothetically increase the level of expression and the mean fluorescence

beyond what was observed in the single Y238F mutant, which presented the strongest effects in terms of protein expression. In this case, perhaps S246A would not have a major influence on expression levels, since the other two mutants T252A and Y238F are highly expressed. Next, luciferase assays with the luciferase gene under the control of a NKX6-2 response element should be carried out to evaluate the actual role of PTMs in NKX6-2 transcriptional activity.

As mutations in the TAD clearly modify the levels of the NKX6-2 protein, these effects may be indicative of a general relevance of the charges or structure of this domain in the stability of the protein, therefore developing mutants at other sites with S, T and Y residues or even in other amino acids it would be interesting to observe expression levels across the entire domain. As a continuation of the work developed in this thesis and in the article [81], we can explore the effect of NKX6-2 PTMs on the stability and aggregation of the protein, as several mutations related to SPAX8 have already been described and analyzed, some of them with low expression levels and others that cause aggregates. One way to do this would be to develop SPAX8-related mutants that are also mutated to mimic or inhibit phosphorylation at the specific points we have already studied.

5

CONCLUSIONS

The results of our study lead us to the following conclusions:

- NKX6-2 phosphorylation does not regulate its nuclear localization.
- Mutations that affect the TAD domain substantially increase NKX6-2 protein levels, suggesting a role for this domain in the stability or degradation of this protein.
- Overexpression of NKX6-2 and some PTM mutants induces anomalies in nuclear morphologies.
- HeLa, 10B1, HMC3 and C6 cell lines express endogenous NKX6-2.

BIBLIOGRAPHY

[1] Drake, R. L., Vogl, W., Mitchell, A. W. M., & Gray, H. (2019). *Gray's Anatomy for Students* (4th ed.). Elsevier.

[2] Jotz, G., da Silva, M. V. M., dos Santos, P. R., & Silva, L. F. (2017). *Neuroanatomia Clínica e Funcional* (1st ed.). Elsevier.

[3] Schmahmann, J. D. (2004). Disorders of the Cerebellum: Ataxia, Dysmetria of Thought, and the Cerebellar Cognitive Affective Syndrome. *The Journal of Neuropsychiatry and Clinical Neurosciences*, 16(3), 367-378. https://doi.org/10.1176/jnp.16.3.367.

[4] Schmahmann, J. D., & Caplan, D. (2006). Cognition, emotion, and the cerebellum. *Brain*, 129, 290–292. https://doi.org/10.1093/brain/awh729.

[5] Ito, M. (2008). Control of mental activities by internal models in the cerebellum. *Nature Reviews Neuroscience*, 9, 304-313. https://doi.org/10.1038/nrn2332.

[6] Schuenke, M., Schulte, E. & Schumacher, U. (2020). Atlas of Anatomy: *Head, Neck and Neuroanatomy* (3rded.). Thieme.

[7] Leitner, Y., Travis, K. E., Ben-Shachar, M., Yeom, K. W. & Feldman, H. M. (2015). Tract profiles of the cerebellar white matter pathways in children and adolescents. *Cerebellum*, 14(6), 613-623. https://doi.org/10.1007/s12311-015-0652-1.

[8] Colin, F., Ris, L., & Godaux, E. (2010). Neuroanatomy of the cerebellum. In M. Manto & M. Pandolfo (Eds.), *The Cerebellum and its Disorders* (pp. 6–29). Cambridge University Press. https://doi.org/10.1017/CBO9780511666469.

[9] D'Angelo, E. (2018). Physiology of the cerebellum. In M. Manto & T. A. G. Huisman (Eds.), *The Cerebellum: From Embryology to Diagnostic Investigations* (1st ed. pp. 85-108). Elsevier.

[10] Haines, D. E. & Mihailoff, G. A. (2018). *Fundamental Neuroscience for Basic and Clinical Applications* (5th ed.). Elsevier.

[11] Manto, M. (2022). The underpinnings of cerebellar ataxias. *Clinical Neurophysiology Practice*, 7, 372-387. https://doi.org/10.1016/j.cnp.2022.11.002.

[12] Ovalle, W. K. & Nahirney, P. C. (2014). *Netter Bases da Histologia* (2nd ed.). Elsevier.

[13] Brinke, M. M, Boele, H. J. & Zeeuw, C. I. (2019). Conditioned climbing fiber responses in cerebellar cortex and nuclei. *Neuroscience Letters* 688, 26-36. https://doi.org/10.1016/j.neulet.2018.04.035.

[14] Lahunta, A. & Glass, E. (2008). Cerebellum. *Veterinary Neuroanatomy and Clinical Neurology,* (3rd ed., Vol 13, pp. 348-388).

[15] Malicki, M., Szmyd, B. M., Bobeff, E. J., Karuga, F. F., Piotrowski, M. M., Kościołek, D., Wanibuchi, S., Radek, M & Jaskólski, D. J. (2023). The Superior Cerebellar Artery: Variability and Clinical Significance. *Biomedicines* 11(7). https://doi.org/10.3390/biomedicines11072009.

[16] Muhammad, S., Hafez, A., Kaukovalta, H., Jahromi, B. R., Kivisaari, R., Hänggi, D. & Niemelä, M. (2023). Anterior inferior cerebellar artery (AICA) aneurysms: a radiological study of 15 consecutive patients. *Frontiers in Radiology*, 3. https://doi.org/10.3389/fradi.2023.1229921.

[17] Junior, Z. D., Guimarães, R. M. R., Vialle, E. N., Koppe, G. L., Francisco, A. N. & Gatto, L. A. M. (2019). Origin of the Posterior Inferior Cerebellar Artery over the C1 Posterior Arch. *Revista Brasileira de Ortopedia e Traumatologia*, 54(5), 605-608. https://doi.org/10.1016/j.rbo.2017.12.025.

[18] Woodward, K., Apps, R., Goodfellow, M., Cerminara, N. L. (2022). Cerebello-Thalamo-Cortical Network Dynamics in the Harmaline Rodent Model of Essential Tremor. *Frontiers in Systems Neuroscience*, 16. https://doi.org/10.3389/fnsys.2022.899446.

[19] Ustárroz, J. T., Lario, P.L., Fernàndez, M. D. I. & Goñi, P. H. (2011). Contribución del cerebelo a los procesos cognitivos: avances actuales. *Revista de Neurología*, 53(5), 301-315. https://doi.org/10.33588/rn.5305.2010747.

[20] Schmahmann, J. D. (2019). The cerebellum and cognition. *Neuroscience Letters*, 688, 62-75. https://doi.org/10.1016/j.neulet.2018.07.005.

[21] Witek, N., Hawkins, J. & Hall, D. (2021). Genetic ataxias: update on classification and diagnostic approaches. *Current Neurology and Neuroscience Reports,* 21(3). https://doi.org/10.1007/s11910-021-01092-4.

[22] Brent, L. & Fogel, M.D. (2012). Childhood Cerebellar Ataxia. *Journal of Child Neurology* 27(9). https://doi.org/10.1177/0883073812448231.

[23] Beaudin, M., Klein, C. J., Rouleau, G. A. & Dupré, N. (2017). Systematic review of autosomal recessive ataxias and proposal for a classification. *Cerebellum ataxias*, 23(4). https://doi.org/10.1186/s40673-017-0061-y.

[24] Tsuji, S. (2013). Idiophatic Late Onset Cerebellar Ataxia (ILOCA), and Cerebellar plus Syndrome. In M. Manto, D. L. Gruol, J. D. Schmahmann, N. Koibuchi & F. Rossi (Eds.), *Handbook of the Cerebellum and Cerebellar Disorders* (pp. 2143-2150). Springer.

[25] Nemeth, A. H., Kwasniewska, A. C., Lise, S., Parolin, R. S., Becker, E. B., Bera, K. D., Shanks, M. E., Gregory, L., Buck, D., Cader, M. Z., Talbot, K., de Silva, R., Fletcher, N., Hastings, R., Jayawant, S., Morrison, P. J., Worth, P., Taylor, M., Tolmie, J., O'Regan, M., Valentine, R., Packham, E., Evans, J., Seller, A. & Ragoussis, J. (2013). Next generation sequencing for molecular diagnosis of neurological disorders using ataxias as a model. *Brain,* 136(10), 3106-3118. https:/doi.org/10.1093/brain/awt236.

[26] Behjati, S., Tarpey, P. S. (2013). What is next generation sequencing? *Archives of Disease in Childhood*, 98(6), 236-238. https://doi.org/10.1136/archdischild-2013-304340.

[27] Trouillas, P., Takayanagi, T., Hallett, M., Currier, R. D., Subramony, S. H., Wessell, K., Bryer, A., Diener, H. C., Massaquoi, S., Gomez, C. M., Coutinho, P., Hamida, M. B., Campanella, G., Filla, A., Schut, L., Timann, D., Honnorat, J., Nighoghossian, N. & Manyam, B. (1997). International Cooperative Ataxia Rating Scale for pharmacological assessment of the cerebellar syndrome. *Journal of the Neurological Sciences* 145:2, 205-211. https://doi.org/10.1016/s0022-510x(96)00231-6.

[28] Schmitz-Hübsch, T., du Montcel, S. T., Baliko, L., Berciano, J., Boesch, S., Depondt, C., Giunti, P., Globas, C., Infante, J., Kang, J-S., Kremer, B., Mariotti, C., Melegh, B., Pandolfo, M., Rakowicz, M., Ribai, P., Rola, R., Schols, L., Szymanski, S., van de Warrenburg, B. P., Dürr, A., Klockgether, T. & Fancellu, R. Scale for the assessment and rating of ataxia: development of a new clinical scale. (2006). *Neurology*, 66(11), 1717-1720. https://doi.org/10.1212/01.wnl.0000219042.60538.92.

[29] Schmahmann, J. D., Gardner, R., MacMore, J. & Vangel, M. G. (2009). Development of a brief ataxia rating scale (BARS) based on a modified form of the ICARS. *Movement Disorders,* 24(12), 1820-1828. https://doi.org/ 10.1002/mds.22681.

[30] Blumenfeld, H. (2010). Neuroanatomy trough clinical cases (2nd ed.). *Sunderland*.

[31] Bonneau, D., Colin, E., Oca, F., Ferre, M., Chevrollier, A., Gueguen, N., Desquiret- Dumas, V., N'Guyen, S., Barth, M., Zanlonghi, X., Rio, M., Desguerre, I., Barnerias, C., Momtchilova, M., Rodriguez, D., Slama, A., Lenaers, G., Procaccio, V., Amati-Bonneau, P. & Reynier, P. (2014). Early-onset Behr syndrome due to compound heterozygous mutations in OPA1. *Brain*, 137(10), e301. https://doi.org/ 10.1093/brain/awu184.

[32] Ruano, L., Melo, C., Silva, M. C. & Coutinho, P. (2014). The global epidemiology of hereditary ataxia and spastic paraplegia: a systematic review of prevalence studies. *Neuroepidemiology,* 42(3), 174-183. https://doi.org/10.1159/000358801.

[33] Coutinho, P., Ruano, L., Loureiro, J. L., Cruz, V. T., Barros, J., Tuna, A., Barbot, C., Guimarães, J., Alonso, I., Silveira, I., Sequeiros, J., Neves, J. M., Serrano, P. & Silva, C. (2013). Hereditary Ataxia and Spastic Paraplegia in Portugal: A Population-Based Prevalence Study. *JAMA Neurology*, 70(6), 746-755. https://doi.org/10.1001/jamaneurol.2013.1707.

[34] Klockgether, T., Mariotti, C. & Paulson, H.L. (2019). Spinocerebellar ataxia. *Nature Reviews Disease Primers* 5(24). https://doi.org/10.1038/s41572-019-0074-3.

[35] Tsuji, S. (2012). Dentatorubral-pallidoluysian atrophy. *Handbook of Clinical Neurology* (Vol. 103, pp. 587-594). Elsevier.

[36] Coutinho, P., Barbot, C. (2002). Ataxia with Oculomotor Apraxia Type 1. In M. P. Adam, G. M. Mirzaa, R. A. Pagon, S. E. Wallace, L. J. H. Bean, K. W. Gripp & A. Amemiya (Eds.), *Gene Reviews*. University of Washington Press.

[37] Cook, A., Giunti, P. (2017). Friedrich's ataxia: clinical features, pathogenesis, and management. *British Medical Bulletin*, 124(1), 19-30. https://doi.org/10.1093/bmb/ldx034.

[38] Ho□zer, R. M. & Matté, C. (2017). Podcasts in Biochemistry and Molecular Biology. *Journal of Biochmistry Education,* 15, 107-125. https://doi.org/10.16923/reb.v15i0.684.

[39] Chelban, V., Kaya, N., Alkuraya, F. & Houlden, H. (2018). NKX6-2-Related Disorder. *Gene Reviews*.

[40] Chelban, V., Alsagob, M., Kloth, K., Chirita-Emandi, A., Vandrovcova, J., Maroofian, R., Davagnanam, I., Bakhtiari, S., AlSayed, M. D., Rahbeeni, Z., AlZaidan, H., Malintan, N. T.,

Johannsen, J., Efthymiou, S., Ghayoor Karimiani, E., Mankad, K., Al-Shahrani, S. A., Beiraghi Toosi, M., AlShammari, M., Groppa, S., Haridy, N. A., AlQuait, L., Qari, A., Huma, R., Salih, M. A., Almass, R., Almutairi, F. B., Hamad, M. H., Alorainy, I. A., Ramzan, K., Imtiaz, F., Puiu, M., Kruer, M. C., Bierhals, T., Wood, N. W., Colak, D., Houlden, H. & Kaya, N. (2020). Genetic and phenotypic characterization of NKX6-2-related spastic ataxia and hypomyelination. *European Journal of Neurology,* 27(2), 334-342. https://doi.org/ 10.1111/ene.14082.

[41] Dorboz, I., Aiello, C., Simons, C., Stone, R. T., Niceta, M., Elmaleh, M., Abuawad, M., Doummar, D., Bruselles, A., Wolf, N. I., Travaglini, L., Boespflug-Tanguy, O., Tartaglia, M., Vanderver, A., Rodriguez, D., Bertini, E. (2017). Biallelic mutations in the homeodomain of NKX6-2 underlie a severe hypomyelinating leukodystrophy. *Brain*, 140(10), 2550-2556. https://doi.org/ 10.1093/brain/awx207.

[42] Ramazi, S. & Zahiri, J. (2021). Post-translational modifications in proteins: resources, tools, and prediction methods. *Database: The Journal of Biological Databases and Curation*, 2021. https://doi.org/10.1093/database/baab012.

[43] Southwood, C., He, C., Garbern, J., Kamholz, J., Arroyo, E., Gow, A. (2004). CNS myelin paranodes require Nkx6-2 homeoprotein transcriptional activity for normal structure. *Journal of Neuroscience Research*, 24, 11215–11225. https://doi.org/10.1523/JNEUROSCI.3479-04.2004.

[44] Zheng, Y., Huang, Q., Ding, Z., Liu, T., Xue, C., Sang, X. & Gu, J. (2016). Genome-wide DNA methylation analysis identifies candidate epigenetic markers and drivers of hepatocellular carcinoma, Briefings in Bioinformatics, 19(1), 101-108. https://doi.org/10.1093/bib/bbw094.

[45] Aung, M. T., Bakulski, K. M., Feinberg, J. I., Dou, J. F., Meeker, J. D., Mukherjee, B., Loch-Caruso, R., Ladd-Acosta, C., Volk, H. E., Croen, L. A., Hertz-Picciotto, I., Newschaffer, C. J. & Fallin, M. D. (2022). Maternal blood metal concentrations and whole blood DNA methylation during pregnancy in the Early Autism RiskLongitudinal Investigation (EARLI). *Epigenetics*, 17, 253-268. https://doi.org/10.1080/15592294.2021.1897059.

[46] Chelban, V., Patel, N., Vandrovcova, J., Zanetti, M. N., Lynch, D. S., Ryten, M., Botía, J. A., Bello, O., Tribollet, E., Efthymiou, S., Davagnanam, I., Bashiri, F. A., Wood, N. W., Rothman, J. E., Alkuraya, F. S. & Houlden, H. (2017). Mutations in NKX6-2 cause progressive spastic ataxia and hypomyelination. *The American Journal of Human Genetics*, 100(6), 969-977. https://doi.org/ 10.1016/j.ajhg.2017.05.009.

[47] Almatrafi, A., Umair, M., Eldardear, A., Al-Luqmani, M., Hashmi, J. A., Albalawi, A. M., Alfadhel, M., Ramzan, K. & Basit, S. (2020). A homozygous missense variant in the homeobox domain of the *NKX6-2* results in progressive spastic ataxia type 8 associated with lower limb weakness and neurological manifestations. *The Journal of Gene Medicine*, 22(8). https://doi.org/10.1002/jgm.3196.

[48] Shurrab, S., Cordeiro, D., Mercimek-Andrews, S. & Shuen, A. Y. (2023). NKX6-2 Disease in Two Unrelated Patients with Early-Onset Spastic Quadriplegia and Diffuse Hypomyelinating Leukodystrophy. *Brain Disorders*, 9. https://doi.org/10.1016/j.dscb.2023.100069.

[49] Li, B., Xiao, H., Pei, Z., Chang, Y., Liu, F. & Wang, L. (2022). Spastic ataxia type 8 with a homozygous mutation of the NKX6-2 gene: a case report and literature review. *Chinese Journal of Applied Clinical Pediatrics*, 24, 456-459.

[50] Stanfel, M. N., Moses, K. A., Schwartz, R. J. & Zimmer, W. E. (2005). Regulation of organ development by the NKX-homeodomain factors: an NKX code. *Cellular and molecular biology*, 51.

[51] Nimura, K., Ura, K., Shiratori, H., Ikawa, M., Okabe, M., Schwartz, R. J. & Kaneda, Y. (2009). A histone H3 lysine 36 trimethyltransferase links Nkx2-5 to Wolf–Hirschhorn syndrome. *Nature,* 460(7252), 287-291. https://doi.org/10.1038/nature08086.

[52] Tamashiro, D. A. A., Alarcon, V. B. & Marikawa, Y. (2012). Nkx1-2 is a transcriptional repressor and is essential for the activation of Brachyury in P19 mouse embryonal carcinoma cell. *Differentiation*, 83(5), 282-292. https://doi.org/10.1016/j.diff.2012.02.010.

[53] Simon, R., Lufkin, T. & Bergemann, A. D. (2007). Homeobox gene Sax2 deficiency causes an imbalance in energy homeostasis. *Developmental dynamics,* 236(10), 2792-2799. https://doi.org/10.1002/dvdy.21320.

[54] Simon, R., Britsch, S. & Bergemann, A. (2011). Ablation of Sax2 gene expression prevents diet-induced obesity. *The FEBS journal,* 278(2), 371-382. https://doi.org/10.1111/j.1742-4658.2010.07960.x.

[55] Yamaguchi, T., Hosono, Y., Yanagisawa, K. & Takahashi, T. (2013). NKX2-1/TTF-1: an enigmatic oncogene that functions as a double-edged sword for cancer cell survival and progression. *Cancer cell,* 23(6), 718-723. https://doi.org/10.1016/j.ccr.2013.04.002.

[56] Attarian, S. J., Leibbel, S. L., Yang, P., Alfano, D. N., Hackett, B. P., Cole, F. S. & Hamvas, A. (2018). Mutations in the thyroid transcription factor gene NKX2-1 result in decreased expression of SFTPB and SFTP. *Pediatric Research,* 84(3), 419–425. https://doi.org/10.1038/pr.2018.30.

[57] Mariyath, M. P., Shahi, M. H., Farheen, S., Tayyab, M., Khanam, N. & Ali, A. (2020). Novel Homeodomain Transcription Factor Nkx2.2 in the Brain Tumor Development. *Current Cancer Drug Targets,* 20(5), 335-340. https://doi.org/10.2174/1568009618666180102111539.

[58] Nagel, S., Pommerenke, C., Meyer, C. & MacLeod, R. (2021). NKL Homeobox Genes NKX2-3 and NKX2-4 deregulate megakaryocytic-erythroid cell differentitation in AML. *International Journal of Molecular Sciences*, 22(21). https://doi.org/10.3390/ijms222111434.

[59] Bouveret, R., Waardenberg, A. J., Schonrock, N., Ramialison, M., Doan, T., de Jong, D., Bondue, A., Kaur, G., Mohamed, S., Fonoudi, H., Chen, C. M., Wouters, M. A., Bhattacharya, S., Plachta, N., Dunwoodie, S. L., Chapman, G., Blanpain, C. & Harvey, R. P. (2015). NKX2-5 mutations causative for congenital heart disease retain functionality and are directed to hundreds of targets. *eLife*, 4. https://doi.org/10.7554/eLife.06942.

[60] Nikolova, M., Chen, X. & Lufkin, T. (1998). Nkx2.6 expression is transiently and specifically restricted to the branchial region of pharyngeal-stage mouse embryos. *Mecanisms of Development,* 69(1-2), 215-218. https://doi.org/10.1016/S0925-4773(97)00174-3.

[61] Zhou, Z., Xiong, L., Wu, Z., Jiang, L., Li, Y., Li, Z., Peng, Y., Ning, K., Zou, X., Liu, Z., Wang, J., Li, Z., Zhou, F., Liu, Z., Zhang, Z. & Yu, C. (2022). NKX2.8 promotes chemosensitivity in bladder urothelial carcinoma via transcriptional repression of MDR1. *Cell Death & Disease*, 13(492). https://doi.org/10.1158/0008-5472.CAN-17-1545.

[62] Kim, M. J., Bhatia-Gaur, R., Banach-Petrosky, W. A., Desai, N., Wang, Y., Hayward, S. W., Cunha, G. R., Cardiff, R. D., Shen, M. M. & Abate-Shen, C. (2002). Nkx3. 1 mutant mice recapitulate early stages of prostate carcinogenesis. *Cancer research*, 62(11), 2999-3004.

[63] Provot, S., Kempf, H., Murtaugh, L. C., Chung, U. I., Kim, D. W., Chyung, J., Kronenberg, H. M. & Lassar, A. B. (2006). Nkx3. 2/Bapx1 acts as a negative regulator of chondrocyte maturation. *Development*, 133(4), 651-662. https://doi.org/10.1242/dev.02258.

[64] Verzi, M. P., Stanfel, M. N., Moses, K. A., Kim, B-M., Zhang, Y., Schwartz, R. J., Shivdasani, R. A. & Zimmer, W. E. (2009). Role of the homeodomain transcription factor Bapx1 in mouse distal stomach development. *Gastroenterology*, 136(5), 1701-1710. https://doi.org/10.1053/j.gastro.2009.01.009.

[65] Aigha, I. I. & Abdelalim, E. M. (2020). NKX6.1 transcription factor: a crucial regulator of pancreatic β cell development, identity, and proliferation. *Stem Cell Research & Therapy*, 11(1), 459. https://doi.org/10.1186/s13287-020-01977-0.

[66] Henseleit, K. D., Nelson, S. B., Kuhlbrodt, K., Hennings, J. C., Ericson, J. & Sander, M. (2005). NKX6 transcription factor activity is required for α- and β-cell development in the pancreas. *Development*, 132(13), 3139-3149. https://doi.org/10.1242/dev.01875.

[67] Moreno-Bravo, J. A., Perez-Balaguer, A. & Martinez, S., Puelles, E. (2010). Dynamic expression patterns of NKX6.1 and NKX6.2 in the developing mes-diencephalic basal plate. *Developmental Dynamics*, 239(7), 2094-2101. https://doi.org/10.1002/dvdy.22327.

[68] Ma, P., Xia, Y., Ma, L., Zhao, S. & Mao, B. (2013). Xenopus NKX6.1 and NKX6.2 are required for mid-hindbrain boundary development. *Development Genes and Evolution*, 223(4), 253-259. https://doi.org/10.1007/s00427-013-0437-9.

[69] Cai, J., Zhu, Q., Zheng, K., Li, H., Qi, Y., Cao, Q. & Qiu, M. Co-localization of Nkx6.2 and Nkx2.2 Homeodomain Proteins in Differentiated Myelinating Oligodendrocytes. *Glia*, 58(4), 458-468. https://doi.org/ 10.1002/glia.20937.

[70] Awatramani, R., Scherer, S., Grinspan, J., Collarini, E., Skoff, R., O'Hagan, D., Garbern, J. & Kamholz, J. (1997). Evidence that the homeodomain protein Gtx is involved in the regulation of oligodendrocyte myelination. *Journal of Neuroscience Research*, 17(17), 6657-6668. https://doi.org/10.1523/JNEUROSCI.17-17-06657.1997.

[71] Liu, R., Cai, J., Hu, X., Tan, M., Qi, Y., German, M., Rubenstein, J., Sander, M. & Qiu, M. (2003) Region-specific and stage-dependent regulation of Olig gene expression and oligodendrogenesis by NKX6-1 homeodomain transcription factor. Development 130(25), 6221–6231. https://doi.org/10.1242/dev.00868.

[72] Yoon, J. H., Eun, J. W., Choi, W. S., Kim, O., Nam, S. W., Lee, J. Y. & Park, W. S. (2016). NKX6.3 is a transcription factor for Wnt/β-catenin and Rho-GTPase signaling-related genes to suppress gastric cancer progression. *EBioMedicine*, 9(97), 97-109. https://doi.org/10.1016/j.ebiom.2016.05.027.

[73] Martin, F. J., Amode, M. R., Aneja, A., Austine-Orimoloye, O., Azov, A. G., Barnes, I., Becker, A., Bennett, R., Berry, A., Bhai, J., Bhurji, S. K., Bignell, A., Boddu, S., Lins, P. R. B., Brooks, L., Ramaraju, S. B., Charkhchi, M., Cockburn, A., Da Rin Fiorretto, L., *et al*. (2023). Ensembl 2023. *Nucleic Acids Research*, 51.D1, D933-D941. https://doi.org/10.1093/nar/gkac958.

[74] Komuro, I., Schalling, M., Jahn, L., Bodmer, R., Jenkins, N. A., Copeland, N. G. & Izumo, S. (1993). Gtx: a novel murine homeobox-containing gene, expressed specifically in glial cells of the brain and germ cells of testis, has a transcriptional repressor activity in vitro for a serum-inducible promoter. *The EMBO journal*, 12(4), 1387-1401. https://doi.org/10.1002/j.1460-2075.1993.tb05783.x.

[75] The UniProt Consortium, UniProt: The Universal Knowledgebase in 2023. *Nucleic acids* research, 51(D1), D523-D531. https://doi.org/10.1093/nar/gkac1052.

[76] Bienert, S., Waterhouse, A., de Beer, T. A. P., Tauriello, G., Studer, G., Bordoli, L. & Schwede, T. (2017). The SWISS-MODEL Repository—new features and functionality. *Nucleic acids research*, 45(D1), D313-D319. https://doi.org/10.1093/nar/gkw1132.

[77] Jumper, J., Evans, R., Pritzel, A., Green, T., Figurnov, M., Ronneberger, O., Tunyasuvunakool, K., Bates, R., Žídek, A., Potapenko, A., Bridgland, A., Meyer, C., Kohl, S. A. A., Ballard, A. J., Cowie, A., Romera-Paredes, B., Nikolov, S., Jain, R., Adler, J., Back, T., Petersen, S., Reiman, D., Clancy, E., Zielinski, M., Steinegger, M., Pacholska, M., Berghammer, T., Bodenstein, S., Silver, D., Vinyals, O., Senior, A. W., Kavukcuoglu, K., Kohli, P. & Hassabis, D. (2021). Highly accurate protein structure prediction with AlphaFold. *Nature*, 596, 583-589. https://doi.org/ 10.1038/s41586-021-03819-2.

[78] Kissinger, C. R., Liu, B. S., Martin-Blanco, E., Kornberg, T. B. & Pabo, C.O. (1990). Crystal structure of an engrailed homeodomain-DNA complex at 2.8 A resolution: A framework for understanding homeodomain-DNA interactions. *Cell*, 63(3), 579-590. https://doi.org/10.1016/0092-8674(90)90453-l.

[79] Gehring, W. J., Müller, M., Affolter, M., Percival-Smith, A., Billeter, M., Qian, Y. Q., Otting, G. & Wüthrich, K. (1990). The structure of the homeodomain and its functional implications. *Trends in Genetics*, 6(10), 323-329. https://doi.org/10.1016/0168-9525(90)90253-3.

[80] Qi, Y., Cai, J., Wu, Y., Wu, R., Lee, J., Fu, H., Rao, M., Sussel, L., Rubenstein, J. & Qiu, M. Control of oligodendrocyte differentiation by the Nkx2.2 homeodomain transcription factor. (2001). *Development*, 128(14). 2723-2733. https://doi.org/10.1242/dev.128.14.2723.

[81] Ferreira-Peralta, P., França, B., Murtinheira, F., Rodrigues, M. S. & Herrera, F. (2023). Is spastic ataxia 8 a proteins misfolding disorder? *Biochimica et Biophysica Acta (BBA) – Molecular Basis of Disease*. https://doi.org/10.1016/j.bbadis.2023.166882.

[82] Karlsson, M., Zhang, C., Méar, L., Zhong, W., Digre, A., Katona, B., Sjöstedt, E., Butler, L., Odeberg, J., Dusart, P., Edfors, F., Oksvold, P., von Feilitzen, K., Zwahlen, M., Arif, M., Altay, O., Li, X., Ozcan, M., Mardinoglu, A., Fagerberg, L., Mulder, J., Luo, Y., Ponten, F., Uhlén, M. & Lindskog, C. (2021). A single-cell type transcriptomics map of human tissues. *Science Advances*, 7(31). https://doi.org/10.1126/sciadv.abh2169.

[83] Wang, D., Eraslan, B., Wieland, T., Hallström, B., Hopf, T., Zolg, D. P., Zecha, J., Asplund, A., Li, L. H., Meng, C., Frejno, M., Schmidt, T., Schnatbaum, K., Wilhelm, M., Ponten, F., Uhlen, M., Gagneur, J., Hahne, H. & Kuster, B. (2019). A deep proteome and transcriptome abundance atlas of 29 healthy human tissues. *Molecular Systems Biology*, 15(2). https://doi.org/10.15252/msb.20188503.

[84] Lee, S. H., Davison, J. A., Vidal, S. M. & Belouchi, A. (2001). Cloning, expression, and chromosomal location of NKX6B TO 10Q26, a region frequently deleted in brain tumors. *Mammalian Genome*, 12(2), 157-162. https://doi.org/10.1007/s003350010247.

[85] Dessaud, E., McMahon, A. P. & Briscoe, J. (2008). Pattern formation in the vertebrate neural tube: a sonic hedgehog morphogen-regulated transcriptional network. *Development*, 135(15), 2489-2503. https://doi.org/10.1242/dev.009324.

[86] Wine-Lee, L., Ahn, K. J., Richardson, R. D., Mishina, Y., Lyons, K. M. & Crenshaw, E. B. (2004). Signaling through BMP type 1 receptors is required for development of interneuron

cell types in the dorsal spinal cord. *Development*, 131(21), 5393-5403. https://doi.org/10.1242/dev.01379.

[87] Rowitch, D.H. & Kriegstein, A.R. (2010). Developmental genetics of vertebrate glial-cell specification. *Nature*, 468(7321), 214-222. https://doir.org/ 10.1038/nature09611.

[88] Briscoe, J., Sussel, L., Serup, P., Hartigan-O'Connor, D., Jessell, T. M., Rubenstein, J. L. & Ericson, J. (1999). Homeobox gene Nkx2.2 and specification of neuronal identity by graded Sonic hedgehog signalling. *Nature*, 398(6728), 622-627. https://doi.org/ 10.1038/19315.

[89] Vallstedt, A., Muhr, J., Pattyn, A., Pierani, A., Mendelson, M., Sander, M., Jessell, T. M. & Ericson, J. (2001). Different levels of repressor activity assign redundant and specific roles to Nkx6 genes in motor neuron and interneuron specification. *Neuron,* 31(5), 743-755. https://doi.org/10.1016/S0896-6273(01)00412-3.

[90] Stifani, N. (2014). Motor neurons and the generation of spinal motor neuron diversity. *Frontiers in Cellular Neuroscience*, 8, 293. https://doi.org/10.3389/fncel.2014.00293.

[91] Awatramani, R., Beesley, J., Yang, H., Jiang, H., Cambi, F., Grinspan, J., Garbern, J. & Kamholz, J. (2000). Gtx, an oligodendrocyte-specific homeodomain protein, has repressor activity. *Journal of Neuroscience Research*, 61(4), 376-387. https://doi.org/10.1002/1097-4547(20000815)61:4<376.

[92] Zhou, Q. & Anderson, D. J. (2002). The bHLH transcription factors OLIG2 and OLIG1 couple neuronal and glial subtype specification. *Cell*, 109(1), 61-73. https://doi.org/10.1016/S0092-8674(02)00677-3.

[93] Vallstedt, A., Klos, J. M. & Ericson, J. (2005). Multiple Dorsoventral Origins of Oligodendrocyte Generation in the Spinal Cord and Hindbrain. *Neuron*, 45(1), 55-67. https://doi.org/10.1016/j.neuron.2004.12.026.

[94] Novitch, B. G., Chen, A. I. & Jessell, T. M. (2001). Coordinate Regulation of Motor Neurons Subtype Identity and Pan-Neuronal Properties by the bHLH Repressor Olig2. *Neuron*, 31(5), 773-789. https://doi.org/10.1016/S0896-6273(01)00407-X.

[95] Zhou, Q., Choi, G. & Anderson, D.J. (2001). The bHLH transcription factor Olig2 promotes oligodendrocyte differentiation in collaboration with Nkx2.2. *Neuron*, 31(5), 791-807. https://doi.org/10.1016/S0896-6273(01)00414-7.

[96] Toch, M., Harris, A., Schakman, O., Kondratskaya, E., Boulland, J-L., Dauguet, N., Debrulle, S., Baudouin, C., Hidalgo-Figueroa, M., Mu, X., Gow, A., Glover, J. C., Tissir, F. & Clotman, F. (2020). Onecut-dependent Nkx6.2 transcription factor expression is required for proper formation and activity of spinal locomotor circuits. *Scientific Reports*, 10(13531). https://doi.org/10.1038/s41598-020-57945-4.

[97] Espana, A. & Clotman, F. (2012). Onecut factors control development of the Locus Coeruleus and of the mesencephalic trigeminal nucleus. *Molelular and Cellular Neuroscience*, 50(1), 93-102. https://doi.org/10.1016/j.mcn.2012.04.002.

[98] Audouard, E., Schakman, O., René, F., Huettl, R-E., Huber, A. B., Loeffler, J-P., Gailly, P. & Clotman, F. (2012). The Onecut transcription factor HNF-6 regulates in motor neurons the formation of the neuromuscular junctions. *PLoS One*, 7(12). https://doi.org/10.1371/journal.pone.0050509.

[99] Harris, A., Masgutova, G., Collin, A., Toch, M., Hidalgo-Figueroa, M., Jacob, B., Corcoran, L. M. & Francius, C. (2019). Onecut Factors and Pou2f2 Regulate the Distribution of V2

Interneurons in the Mouse Developing Spinal Cord. *Frontiers in Celular Neuroscience,* 13(184). https://doi.org/10.3389/fncel.2019.00184.

[100] Huang, K-Y., Lee, T-Y., Kao, H-J, Ma, C-T., Lee, C-C., Lin, T-H., Chang, W-C. & Huang, H-D. (2018). dbPTM in 2019: exploring disease association and cross-talk of post-translational modifications. *Nucleic Acids Research,* 47(D1), D298-D308. https://doi.org/10.1093/nar/gky1074.

[101] Marshall, C. (1993). Protein prenylation: a mediator of protein-protein interactions. *Science*, 259(5103), 1865-1867. https://doi.org/10.1126/science.8456312.

[102] Caragea, C., Sinapov, J., Silvescu, A., Dobbs, D. & Honavar, V. (2007). Glycosylation site prediction using ensembles of Support Vector Machine classifiers. *BMC Bioinformatics*, 8(438). https://doi.org/10.1186/1471-2105-8-438.

[103] Ryšlavá, H., Doubnerová, V., Kavan, D. & Vaněk, O. (2013). Effect of posttranslational modifications on enzyme function and assembly. *Journal of Proteomics*, 92, 80-109. https://doi.org/10.1016/j.jprot.2013.03.025.

[104] Del Monte, F. & Agnetti, G. (2014). Protein post-translational modifications and misfolding: new concepts in heart failure. *Proteomics – Clinical Applications,* 8(7-8), 534-542. https://doi.org/10.1002/prca.201400037.

[105] Reiche, J. & Huber, O. (2020). Post-translational modifications of tight junction transmembrane proteins and their direct effect on barrier function. *Biochimica et Biophysica. Acta (BBA) – Biomembranes,* 1862(9). https://doi.org/10.1016/j.bbamem.2020.183330.

[106] Liu, H., Du, T., Li. C. & Yang, G. (2021). STAT3 phosphorylation in central leptin resistance. *Nutrition & Metabolism,* 18(1), 39. https://doi.org/ 10.1186/s12986-021-00569-w.

[107] Tenreiro, S., Eckermann, K. & Outeiro, T. F. (2014). Protein phosphorylation in neurodegeneration: friend or foe? *Frontiers in Molecular Neuroscience*, 7(42). https://doi.org/10.3389/fnmol.2014.00042.

[108] Bhaskara, G. B., Wong, M. M. & Verslues, P. E. (2019). The flip side of phosphor-signalling: Regulation of protein dephosphorylation and the protein phosphatase 2Cs. *Plant, Cell & Environment*, 42(10), 2913-2930. https://doi.org/10.1111/pce.13616.

[109] Humphrey, S. J., James, D. E. & Mann, M. (2015). Protein Phosphorylation: A Major Switch Mechanism for Metabolic Regulation. *Trends in Endocrinology & Metabolism*, 26(12), 676-687. https://doi.org/10.1016/j.tem.2015.09.013.

[110] Cohen, P. (2002). The origins of protein phosphorylation. *Nature Cell Biology*, 4, E127-E130. https://doi.org/10.1038/ncb0502-e127.

[111] Ma, L., Chen, Z., Erdjument-Bromage, H., Tempst, P. & Pandolfi, P. P. (2005). Phosphorylation and functional inactivation of TSC2 by Erk. Implications for tuberous sclerosis and cancer pathogenesis. *Cell*, 121(2), 179-193. https://doi.org/10.1016/j.cell.2005.02.031.

[112] Huang, J. & Manning, B. D. (2008). The TSC1–TSC2 complex: a molecular switchboard controlling cell growth. *Biochemical Journal*, 412(2), 179-190. https://doi.org/10.1042/BJ20080281.

[113] Nishi, H., Hashimoto, K. & Panchenko, A. R. (2011). Phosphorylation in protein-protein binding: effect on stability and function. *Structure*, 19(12), 1807-1815. https://doi.org/10.1016/j.str.2011.09.021.

[114] Zhang H., Cao X., Tang M., Zhong G., Si Y., Li H., Zhu, F., Liao, Q., Li, L., Zhao, J., Feng, J., Li, S., Wang, C., Kaulich, M., Wang, F., Chen, L., Li, L., Xia, Z., Liang, T., Lu, H., Feng, X. & Zhao, B. (2021). A subcellular map of the human kinome. *ELife*, 10. https://doi.org/10.7554/eLife.64943.

[115] Sacco F., Perfetto L., Castagnoli L. & Cesareni G. (2012). The human phosphatase interactome: an intricate family portrait. *FEBS Letters,* 586(17), 2732-2739. https://doi.org/10.1016/j.febslet.2012.05.008.

[116] Missero, C., Cobellis, G., De Felice, M. & Di Lauro, R. (1998). Molecular events involved in differentiation of thyroid follicular cells. *Molecular and Cellular Endocrinology*, 140(1-2), 37-43. https://doi.org/ 10.1016/s0303-7207(98)00027-6.

[117] Zhang, C., Huang, H., Chen, Z., Zhang, Z., Lu, W. & Qiu, M. (2020). The transcription factor NKX2-2 regulates oligodendrocyte differentiation through domain-specific interactions with transcriptional corepressors. *Journal of Cellular Biochemistry*, 295(7), 1879-1888. https://doi.org/ 10.1074/jbc.RA119.011163.

[118] Sooreshjani, M. A. (2021). Identifying The Versatile Roles of NKX3.1 Phosphorylation to Explore New Castration-Resistant Prostate Cancer Therapy. *Purdue University Graduate School*. Thesis. https://doi.org/10.25394/PGS.14519691.v1.

[119] Chen, H. & Bieberich, C. J. (2005). Structural and functional analysis of domains mediating interaction between NKX-3.1 and PDEF. *Journal of Cellular Biochemistry*, 94(1), 168-177. https://doi.org/ 10.1002/jcb.20297.

[120] Meng, F., Sun, Q., Zhou, D., Li, Q., Han, J., Liu, D. & Yang, J. (2020). Inhibition of Aurora-A improves insulin resistance by ameliorating islet inflammation and controlling interleukin-6 in a diabetic mouse model, *Adipocyte* 9(1), 609-619. https://doi.org/10.1080/21623945.2020.1829851.

[121] Murtinheira, F., Migueis, M., Vilela, R. L., Diallo, M., Quezada, A., Valente, C. A., Oliva, A., Rodriguez, C., Martin, V. & Herrera, F. Sacsin Deletion Induces Aggregation of Glial Intermediate Filaments. (2022). Cells, 11(2), 299. https://doi.org/10.3390/cells11020299.

[122] Schindelin, J., Arganda-Carreras, I., Frise, E., Kaynig, V., Pietzsch, T., Preibisch, S., Rueden, C., Saalfeld, S., Schmid, B., Tinevez, J., White, D. J., Hartenstein, V., Eliceiri, K., Tomancak, P. & Cardona, A. (2012). Fiji: an open-source platform for biological-image analysis. *Nature Methods,* 9, 676-682. https://doi.org/10.1038/nmeth.2019.

[123] M. M. Bradford. (1976). A rapid and sensitive method for the quantitation of microgram quantities of protein utilizing the principle of protein-dye binding. *Analytical Biochemistry,* 72, 248–254. https://doi.org/10.1016/0003-2697(76)90527-3.

[124] Peralta, P. M. F., Restoring NKX6-2 function by protein complementation: a proof-of-concept. (2021). NOVA University Lisbon. Thesis.

[125] Zink, D., Fischer, A. H. & Nickerson, J. A. (2004). Nuclear structure in cancer cells. *Nature reviews* cancer, 4(9), 677-687. https://doi.org/ 10.1038/nrc1430.

[126] Ferenczy, M. W., Johnson, K. R., Steinberg, S. M., Marshall, L. J., Monaco, M. C., Beschloss, A. M., Jensen, P. N. & Major, E. O. (2013). Clonal Immortalized Human Glial Cell Lines Support Varying Levels of JC Virus Infection due to Differences in Cellular Gene Expression. Journal of Neuroimmune Pharmacology, 8(5), 1303-1319. https://doi.org/ 10.1007/s11481-013-9499-8.

[127] Li, H., de Faria, J. P., Andrew, P., Nitarska, J. & Richardson, W. D. (2011). Phosphorylation Regulates OLIG2 Cofactor Choice and the Motor Neuron-Oligodendrocyte Fate Switch. *Neuron*, 69(5), 918-929. https://doi.org/10.1016/j.neuron.2011.01.030.

[128] Salvi, F., Hoermann, B., García, J., Fontanillo, M., Derua, R., Beullens, M., Bollen, M., Barabas, O. & Kõhn, M. (2020). Towards Dissecting the Mechanism of Protein Phosphatase-1 Inhibition by Its C-Terminal Phosphorylation. *ChemBioChem*, 22(5), 834-838. https://doi.org/10.1002/cbic.202000669.

[129] Julien M., Bouguechtouli C., Alik A., Ghouil R., Zinn-Justin S. & Theillet F. X. (2020). Multiple site-specific phosphorylation of IDPs monitored by NMR. *Methods in Molecular Bioogy,* 2141, 793–817. https://doi.org/ 10.1007/978-1-0716-0524-0_41.

[130] Lowery, J., Kuczmarski, E. R., Herrmann, H. & Goldman, R. D. (2015). Intermediate Filaments Play a Pivotal Role in Regulating Cell Architeture and Function. *Journal of Biological Chemistry*, 290(28), 17145-17153. https://doi.org/10.1074/jbc.R115.640359.